2021

Exogenous Introduction of Initiator and Executioner Caspases Results in Different Apoptotic Outcomes

Francesca Anson
University of Massachusetts Amherst

S Thayumanavan
University of Massachusetts Amherst

Jeanne A. Hardy
University of Massachusetts Amherst

Recommended Citation

Anson, Francesca; Thayumanavan, S; and Hardy, Jeanne A., "Exogenous Introduction of Initiator and Executioner Caspases Results in Different Apoptotic Outcomes" (2021). *JACS*. 1484.
https://doi.org/10.1021/jacsau.1c00261

JACS Au
AN OPEN ACCESS JOURNAL OF THE AMERICAN CHEMICAL SOCIETY

pubs.acs.org/jacsau

Article

Exogenous Introduction of Initiator and Executioner Caspases Results in Different Apoptotic Outcomes

Francesca Anson, S. Thayumanavan,* and Jeanne A. Hardy*

Cite This: *JACS Au* 2021, 1, 1240–1256

Read Online

ACCESS | Metrics & More | Article Recommendations | Supporting Information

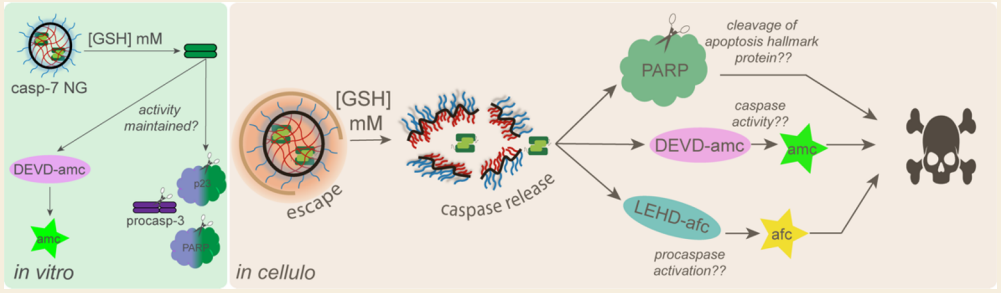

ABSTRACT: The balance of pro-apoptotic and pro-survival proteins defines a cell's fate. These processes are controlled through an interdependent and finely tuned protein network that enables survival or leads to apoptotic cell death. The caspase family of proteases is central to this apoptotic network, with initiator and executioner caspases, and their interaction partners, regulating and executing apoptosis. In this work, we interrogate and modulate this network by exogenously introducing specific initiator or executioner caspase proteins. Each caspase is exogenously introduced using redox-responsive polymeric nanogels. Although caspase-3 might be expected to be the most effective due to the centrality of its role in apoptosis and its heightened catalytic efficiency relative to other family members, we observed that caspase-7 and caspase-9 are the most effective at inducing apoptotic cell death. By critically analyzing the introduced activity of the delivered caspase, the pattern of substrate cleavage, as well as the ability to activate endogenous caspases, we conclude that the efficacy of each caspase correlated with the levels of pro-survival factors that both directly and indirectly impact the introduced caspase. These findings lay the groundwork for developing methods for exogenous introduction of caspases as a therapeutic option that can be tuned to the apoptotic balance in a proliferating cell.

KEYWORDS: *intracellular protein delivery, caspase, intrinsic and extrinsic apoptosis, stimuli-responsive materials, nanogels*

INTRODUCTION

Mutations that block apoptotic cell death accumulate in most cancers, leading to chemoresistance, tumorigenesis, and metastasis.[1] Inducing apoptosis for cancer therapy is a powerful therapeutic strategy, but targeting the appropriate point in the balance between cell death and survival is critical. The apoptotic cascade uses caspases (cysteine aspartate proteases; casp) centrally to cleave a series of substrates resulting in cell death. Apoptotic caspases are classified as either upstream initiator (casp-8 and -9) or downstream executioner (casp-3, -6, and -7), depending on their mechanism and point of activation[2] (Scheme 1). Caspase activation is regulated by pro-survival members of the B-cell lymphoma-2 (Bcl-2) family,[3,4] and caspase activity can be inhibited by inhibitors of apoptotic proteins (IAPs).[4,5] Due to their significant role in apoptosis, suppressed caspase function as well as pro-apoptotic and pro-survival protein imbalance contributes to apoptotic resistance.[6] While virtually all cancers have developed means of evading apoptosis, the mechanism of evasion differs widely between cancers. Thus, increasing the amount of an appropriate active intracellular caspase to induce apoptosis in individual cancer environments is a powerful therapeutic strategy, particularly because caspases are inherently catalytic.

Casp-3 has undoubtedly been the most prevalent apoptotic cargo for exogenous introduction, due to its known apoptotic potency, which stems from a vast substrate pool and the most efficient substrate turnover of all caspases.[7] However, because each cancer has evolved a unique repertoire of blocks to apoptosis, and because each caspase is subject to unique regulation, it is plausible that the identity of the caspase that would be most effective at triggering cell death will depend exquisitely on the unique repertoire of accumulated anti-apoptotic mutations. In addition, after activation, the various caspases show different subcellular distribution among the cytosol, nucleus, microsomes, or mitochondria[8,9] due to their

Received: June 9, 2021
Published: July 8, 2021

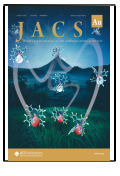

Scheme 1. Exogenous Introduction of Different Apoptotic Caspases May Result in Unique Apoptotic Outcomes[a]

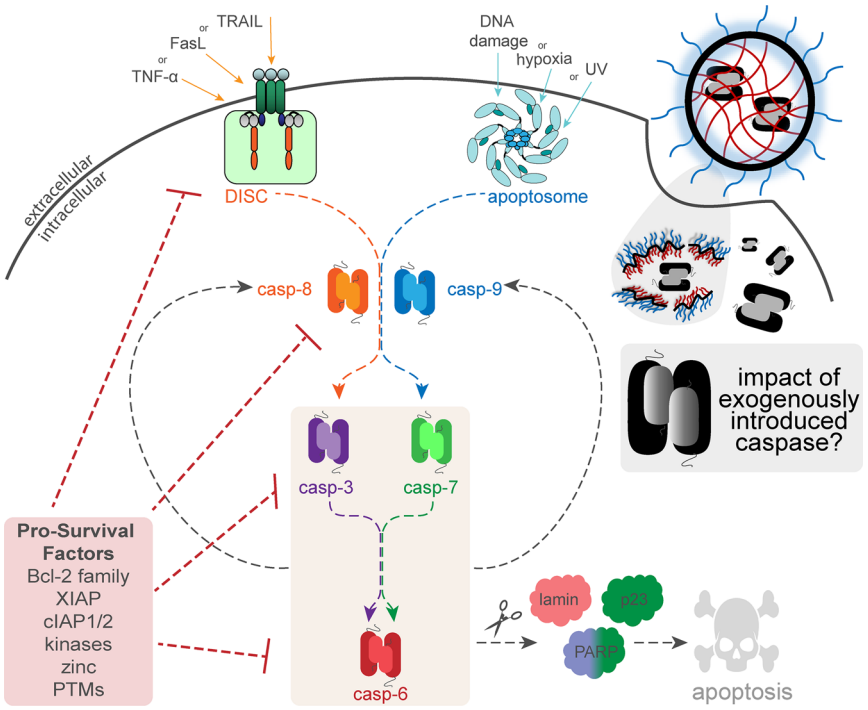

[a]Apoptotic pathways are mediated by caspases, calling into question which exogenously introduced caspase will be most effective at inducing cell death. Initiators casp-8 and casp-9 are activated in response to extrinsic and intrinsic stimuli, respectively. After initiator caspase activation, the executioners casp-3, -6, and -7 are activated, resulting in feedback activation of initiator caspases and direct substrate proteolysis, leading to cell death. Caspase activity is inhibited by pro-survival factors which are overexpressed to various extents in various cancerous tissues. Example executioner caspase substrates include poly(ADP-ribose) polymerase 1 (PARP-1), p23, and lamin A, colored to match the caspase that cleaves them (i.e., red for casp-6, green for casp-7, and green/purple for casp-3 and -7). Exogenous introduction of each of the apoptotic caspases, via nanogel intracellular delivery, allowed us to assess which caspase is best at cleaving cells of a given pro-survival profile.

differential cleavage of elements that control organelle entry. Thus, the ideal caspase for inducing apoptosis in various cancers must be individually evaluated.

The efficacy of introducing exogenous casp-3 has been investigated by our group using redox-responsive polymeric materials[10,11] and others via assorted materials including peptides,[12] lipids,[13] dendrimers,[14] polymers,[15] and inorganics.[16−18] Similarly, casp-3 and casp-9 have been exogenously introduced to cells using gene therapies.[19−21] Introducing the native human casp-3 gene encoding procaspase-3 zymogen has been found to be unproductive without an apoptosis inducer,[20] which is not surprising. To circumvent this, genes encoding a constitutively active, non-native casp-3 are required for any apoptotic efficacy.[21] Gene therapies for an inducible casp-9 have also generated interest, but again, they require cell-permeable molecules for activation,[22] are enhanced with apoptosis inducers,[23] and require tissue-specific promoters to achieve cell-specific expression.[19,24] In addition, delivering cytochrome *c* leads to significant caspase-mediated cell death by stimulating apoptosome formation, suggesting there is merit to fully explore delivery of activated caspases.[25−27]

Here, we utilize redox-responsive polymeric nanogels (NGs) as an accessible biochemical tool to exogenously introduce active casp-3, -6, -7, -8, or -9 into live cells, requiring preparation of only two components: recombinant purification of the caspase of interest and synthesis of the delivery polymer. The polymer used herein,[10] as well as other derivatives,[26,28−30] has been previously reported for a myriad of cargo. After a facile aqueous reaction and purification, caspase NG (casp-NG) addition to serum-containing cell cultures facilitates examination of the apoptotic inducibility of different caspases in cells with diverse anti-apoptotic repertoires. Casp-8 and casp-9 are initiators and are activated upstream in response to extrinsic or intrinsic stimuli, respectively. In the extrinsic pathway, extracellular death ligands (i.e., TRAIL, FasL, TNF-α) trigger the recruitment of zymogen procasp-8 via death effector domain (DED) interactions to the death-inducing signaling complex (DISC), leading to casp-8 activation.[2] In the intrinsic pathway, mitochondrial stress from internal triggers (i.e., sensing of radiation, hypoxia, chemotherapeutics) facilitates the recruitment of procasp-9 via caspase activation and recruitment domain (CARD) interactions to form the apoptosome, activating casp-9.[2] In contrast to the executioners, both casp-8 and casp-9 fail to be maximally activated solely by proteolysis or dimerization, but are fully activated upon formation of multimer protein−protein complexes, likely due to induced proximity-mediated activation.[31,32] Activation of both casp-8 or casp-9 converges in proteolysis of executioner procasp-3 and -7 at their inter-subunit linker (ISL). This cleavage generates the mature, active casp-3 and -7. The presence of active casp-3 and -7 results in procasp-6 cleavage and activation.[33−36] Importantly, upon the activation of the executioner caspases, the intrinsic and extrinsic pathways cross-talk, leading to signal amplification as casp-3 can process procasp-9[37] and casp-6 can directly activate procasp-8.[38] Procaspase activation pathways upon intrinsic[35,39,40] and extrinsic[41−43] stimuli, caspase feedback loops,[34,36,44] and caspase−procaspase proteolysis in vitro[45,46] have been thoroughly investigated (Scheme S1).[33−42] These features highlight

https://doi.org/10.1021/jacsau.1c00261
JACS Au 2021, 1, 1240−1256

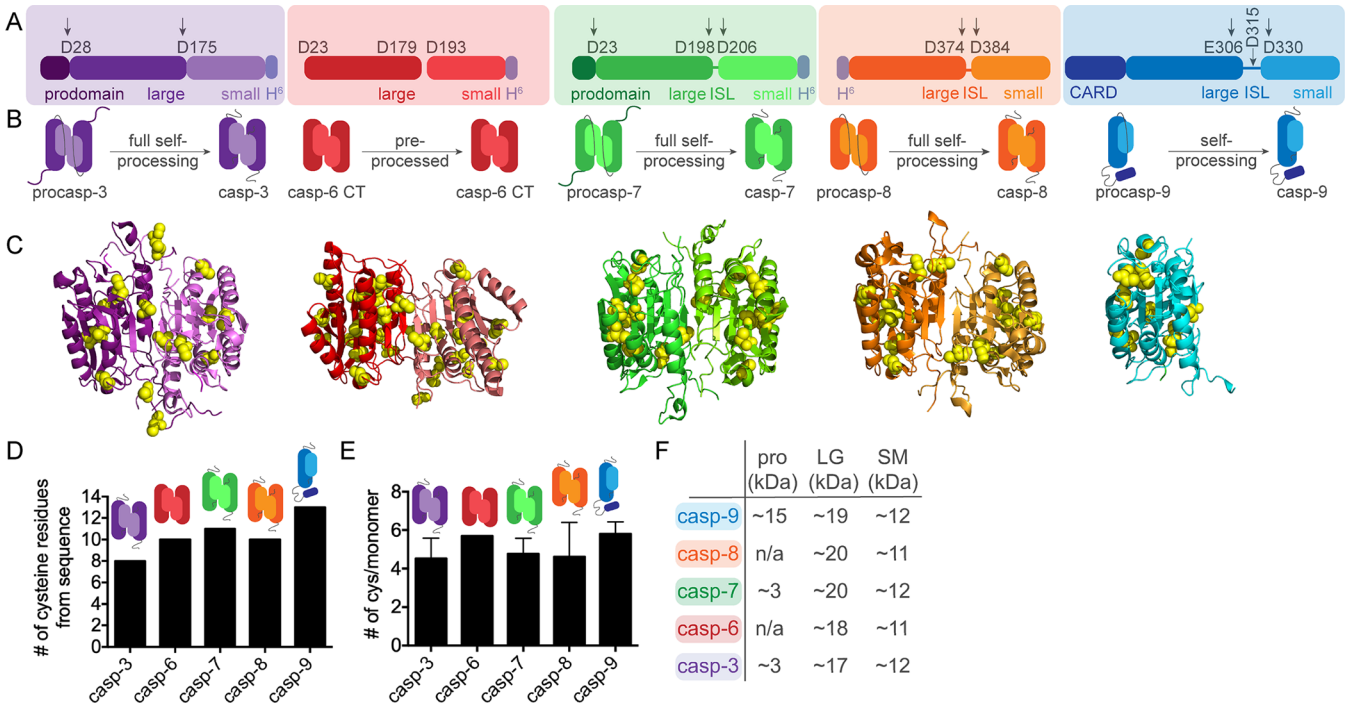

Figure 1. Apoptotic caspase constructs used. (A) Cartoons representing the linear sequence of caspases. Generally, caspase constructs contain a *N*-terminal prodomain followed by a large subunit, intersubunit linker (ISL), and small subunit as well as a hexahistidine (H^6) tag. Gray arrows and corresponding aspartic acid residues represent cleavage sites. Constitutively two-chain (CT) casp-6 does not contain a prodomain nor ISL. (B) Cartoons reflecting caspase self-processing. Large subunits are represented in the dark shade and small subunits in the light shade. (C) Oligomeric caspase structures with cysteine residues highlighted as yellow spheres. Each of the monomers, which are composed of one large and one small subunit after cleavage at the ISL, are drawn in a different shade. PDB IDs: casp-3 (2C2O), casp-6 (3K7E), casp-7 (3IBF), casp-8 (2C2Z), casp-9 (1JXQ). (D) Total number of caspase cysteine residues. (E) Total number of solvent-exposed cysteine residues calculated using Ellman's reagent on two separate days. (F) Tabulated molecular weights of caspase subunits in the constructs used.

the fact that the network by which each caspase might independently induce cell death is distinct.[47] Our ability to deliver different caspases offers a unique opportunity to evaluate the impact of exogenous caspase introduction on cellular fate.

Moreover, the synchronized activation of executioners casp-3, -6, and -7 leads to cleavage of protein substrates critical to intracellular function and cell structure, irreversibly sentencing a cell to death.[48] Casp-3 and -7 share some biochemical similarity as they are observed to recognize the same cleavage motif (DEVD) but are functionally distinct with both overlapping and non-overlapping substrate pools.[40,45] Removal of both enzymes together demonstrates significant resistance to apoptosis upon both intrinsic or extrinsic stimuli, underlying merit for subsequent casp-7 delivery investigation.[36] Casp-6 has canonically been characterized as an apoptosis executioner,[38] with tumor-associated cancer mutations,[49] but its removal has no significant effect on apoptosis.[36] Overall, this study takes a concerted approach to understanding the consequence of polymeric nanogel-based exogenous introduction of different caspases on cellular apoptosis (Scheme 1).

RESULTS AND DISCUSSION

To harness the power of any caspase to induce apoptosis in cells into which they are exogenously introduced, it is important that they are intracellularly delivered in their mature and active forms. For this reason, we used constructs that all produce active (cleaved) caspases: full-length wild-type (WT) casp-3, constitutively two-chain (CT) casp-6, full-length WT casp-7, ΔDED casp-8 (with improved solubility and lower aggregation),[50] and full-length WT casp-9 (Figure 1A). Bacterially overexpressed full-length procaspase-3, -7, -8, and -9 zymogens self-proteolyze, generating the large and small subunits and the properly formed substrate binding groove of the active caspase (Figure 1B). CT casp-6 expresses the large and small subunits independently, mimicking native activation by cleavage.[51] The canonical dimer-of-dimers (heterotetramer) caspase structure is conserved in all caspases (Figure 1B,C), although casp-8 exists as a monomer/dimer mixture[52] and casp-9 exists primarily as a monomer prior to binding substrate.[53] The apoptotic caspases each contain 8−13 cysteines, comprising 3−3.5% of total sequence (Figure 1C,D), with 5−6 thiols solvent exposed (Figure 1E) in each similarly sized caspase (Figure 1F). Thus, delivery vehicle formulation using thiol chemistry is feasibly possible for all caspases as cargo.

Caspases Can Be Stably Encapsulated in PEG−PDS Polymers to Form Casp-NGs

For exogenous introduction of caspases, a compatible delivery vehicle formulation is clearly essential. Our group has created redox-responsive polymers capable of casp-3 encapsulation without any irreversible modification of the protein surface.[10] The amphiphilic random copolymers used here are composed of polyethylene glycol (PEG) and pyridyl disulfide (PDS), the hydrophilic and hydrophobic units, respectively (Figure 2A). In aqueous media, PEG−PDS polymers self-assemble into aggregates that can be cross-linked with a reducing agent (e.g., DTT) to stabilize the nanomaterial.[54] During the polymer self-assembly stage, casp-3 is easily encapsulated via reaction of casp-3's solvent-exposed cysteine residues with polymer PDS units (Figure 2A). Upon NG cellular uptake and endosomal escape,

https://doi.org/10.1021/jacsau.1c00261
JACS Au 2021, 1, 1240−1256

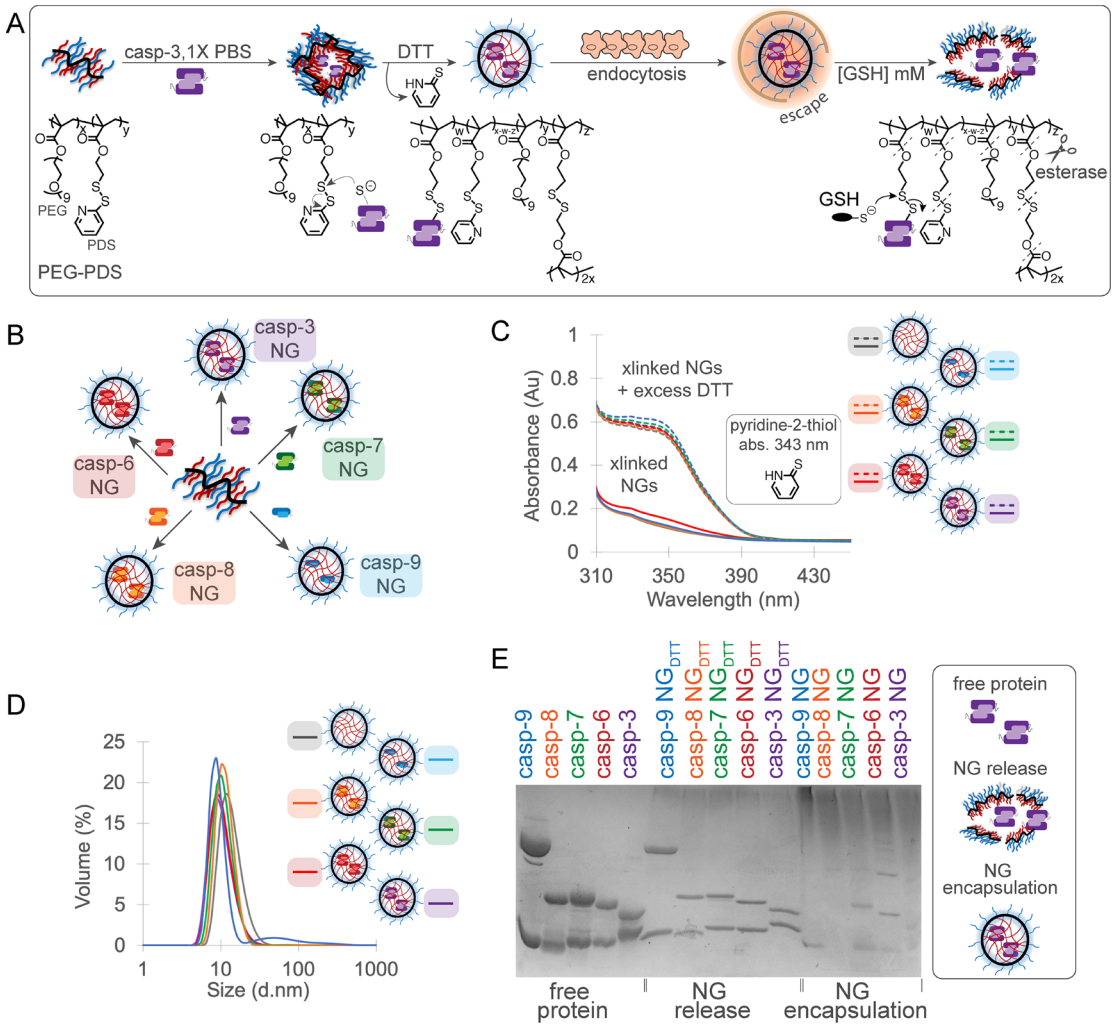

Figure 2. Apoptotic casp-NG formation and characterization. (A) Dissolving amphiphilic PEG−PDS polymers in aqueous milieu results in nanoaggregates that can be cross-linked into stable nanogels by a reducing agent, such as dithiothreitol (DTT). To generate casp-3 NG, casp-3 is added to the aqueous PEG−PDS solution prior to cross-linking. (B) Substituting the different apoptotic caspases in place of casp-3 allows generation of the caspase nanogel (casp-NG) series. (C) Casp-NGs are prepared to ensure formation of similar NG. The degree of cross-linking is quantified by absorbance of pyridine-2-thiol at 343 nm. (D) Casp-NG size distribution. Data show the average of three technical replicates. (E) Casp-NG protein encapsulation and release visualized by comparing caspase subunit intensities using nonreducing and reducing conditions for SDS-PAGE.

intracellular glutathione (GSH) simultaneously reduces the NG cross-links and releases native casp-3, followed by presumed degradation of the remaining material by endogenous esterases (Figure 2A). The casp-NG series (Figure 2B) was generated as previously described[10] using a 1:25 caspase/polymer ratio, with DTT-mediated cross-linking assessed by released pyridine-2-thiol absorbance at 343 nm (Figure 2C).[55] Monodisperse nanomaterials of ∼10 nm were observed for all caspase cargos (Figure 2D). Encapsulation efficiencies were comparable across all cargos (Figure S1), and DTT-mediated release of apoptotic casp-3, -6, -7, -8, and -9 was robustly observed (Figure 2E).

Casp-NG Formation Influences the Activity of Each Caspase toward Peptide Substrates Distinctly

Effective delivery of an enzyme like a caspase requires that both encapsulation and release can be achieved without negatively impacting enzymatic function. We assessed the effect of NG formation on the ability of released caspases to cleave a fluorogenic tetrapeptide substrate in a buffer optimized for each caspase.[56] Casp-3 maintains 80% activity (Figure 3A) of the free casp-3 control.[10] Comparatively, NG-released casp-6 and casp-7 demonstrated significantly more activity (256 ± 31% and 162 ± 11%, respectively) than their free counterparts (Figure 3B,C). Free casp-6 and casp-7 controls showed significant precipitation, whereas casp-6 or -7 NG did not, suggesting that the reactive self-assembly process protected the encapsulated cargo from self-proteolysis and aggregation, as observed for casp-3.[10] In comparison, the initiators, casp-8 and -9, demonstrated minimal proteolytic activity (7 ± 1% and 6 ± 6%, respectively) upon NG release (Figure 3D,E). This loss in activity may be related to the fact that the concentrations of the initiator caspases released from NG are not sufficient to support their proximity-induced activation,[31,32] which is required to increase their inherently low catalytic efficiencies (Table S1). Thus, we hypothesized that a more catalytically active casp-9 variant, constitutively dimeric casp-9 (casp-9_{cD}),[57] might retain more activity following NG formation. Casp-9_{cD} differs from WT casp-9 by only five residues, derived from the casp-3 dimerization interface, which enables casp-9_{cD} to form an active dimer.[57] Casp-9_{cD} demonstrated similar NG encapsulation and release to WT casp-9 (Figure S2). However, NG-released casp-9_{cD} demonstrated 6-fold more activity than NG-released WT casp-9 (36 vs

https://doi.org/10.1021/jacsau.1c00261
JACS Au 2021, 1, 1240−1256

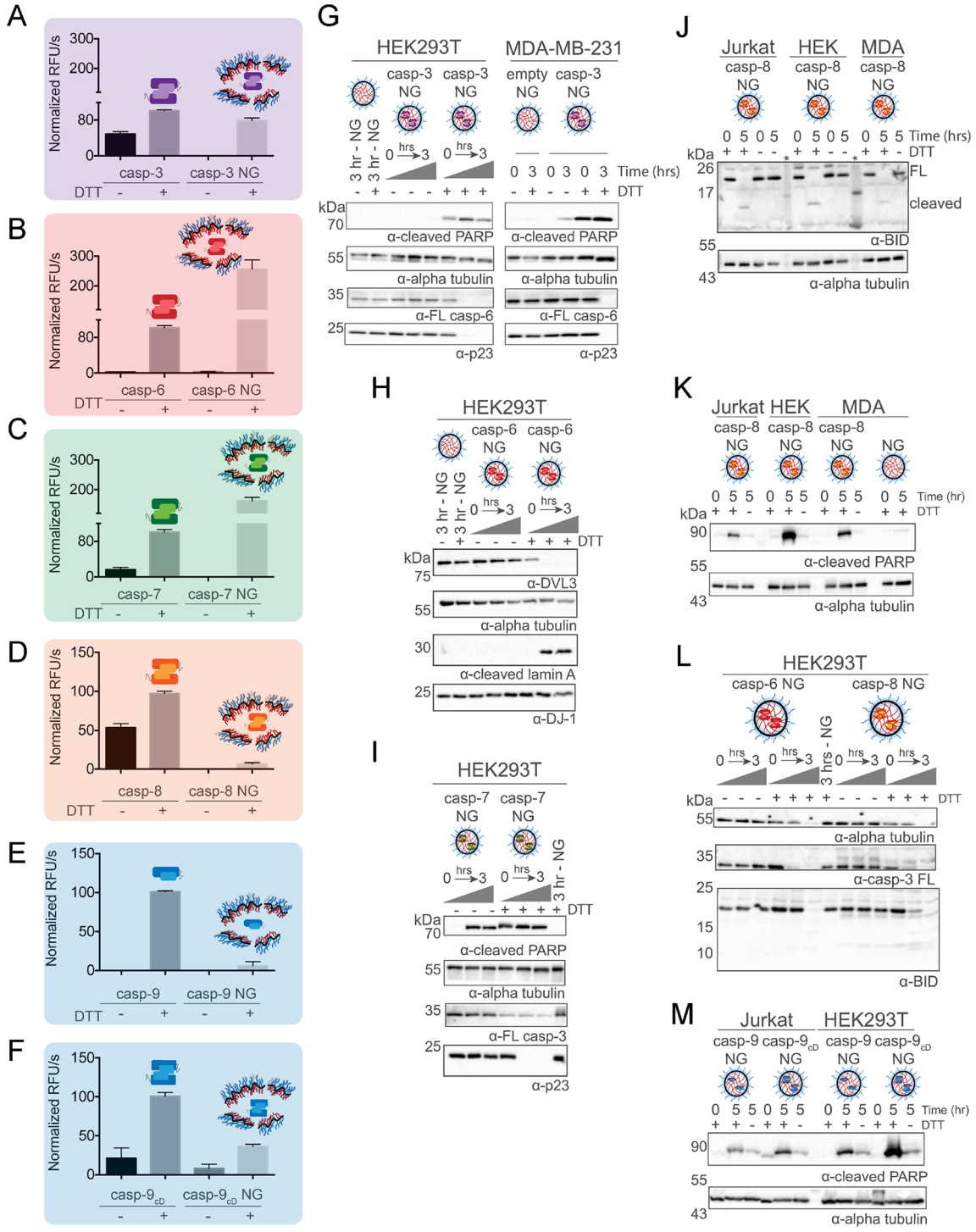

Figure 3. Evaluation of NG-released caspase activity toward peptide and protein substrates. Left lane: NG-released apoptotic caspases demonstrate varying levels of enzymatic activity toward canonical fluorogenic peptide substrates, compared to similarly incubated free protein controls. Casp-NGs were left intact (without DTT) or were added to reductant (with DTT) to facilitate protein release. (A) Casp-3 NG + 100 mM DTT demonstrated 79 ± 6% (average ± SEM) activity of the free protein control toward the fluorogenic peptide substrate DEVD-amc. (B) Casp-6 NG; 256 ± 31%; VEID-afc. (C) Casp-7 NG; 162 ± 11%; DEVD-amc. (D) Casp-8 NG; 7 ± 1%; LEHD-afc. (E) Casp-9 NG; 6 ± 6%; LEHD-afc. (F) Casp-9_{cD} NG; 36 ± 3%; LEHD-afc. All error bars correspond to SEM of three independent NG batches, made and tested on separate days. Western blots: NG-released apoptotic caspases demonstrate cleavage of canonical protein substrates. Casp-NGs were left intact (without DTT) or were added to reductant (with DTT) to facilitate protein release prior to incubation with cell lysates; cell lines include Jurkat T-lymphocytes, embryonic kidney (HEK) cells, and mammary cancer cells (MDA-MB-231). (G) NG-released casp-3-induced cleavage of poly(ADP-ribose) polymerase 1 (PARP-1), full-length (FL) casp-6, and p23 within 3 h. (H) NG-released casp-6-induced cleavage of substrates DVL3, lamin A, and DJ-1 within 1 h. (I) NG-released casp-7-induced cleavage of substrates PARP-1, FL casp-3, and p23 within 1 h. (J) NG-released casp-8-induced cleavage of BH3 interacting domain death agonist after 5 h in three cell lines; *indicates visible ladder (K) NG-released casp-8 also induced cleavage of PARP-1 and (L) executioner FL casp-3 over time. (M) NG-released casp-9-induced PARP-1 cleavage. Immunoblots represent one biological replicate.

https://doi.org/10.1021/jacsau.1c00261
JACS Au 2021, 1, 1240−1256

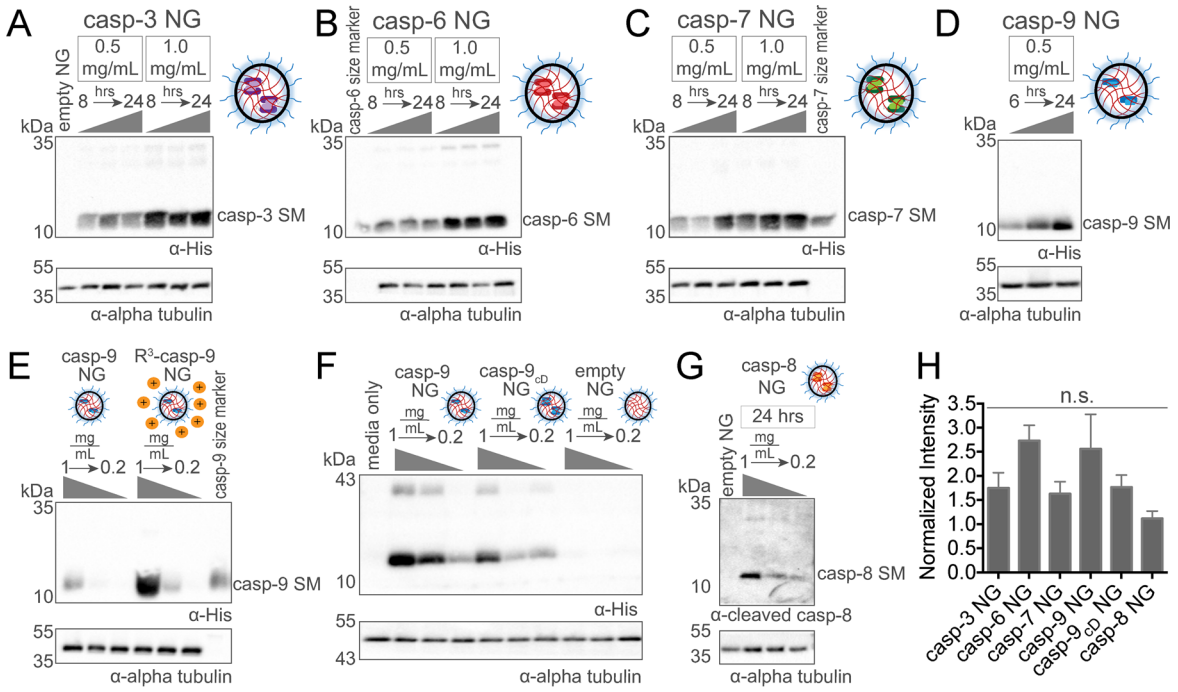

Figure 4. All apoptotic caspases are delivered intracellularly by PEG–PDS NGs. Immunoblot analysis of HEK293T total cell lysate demonstrating efficient PEG–PDS-mediated delivery at different time points. (A) Casp-3 NG, (B) Casp-6 NG, (C) Casp-7 NG, and (D) Casp-9 NG delivery detected using anti-His_6 antibodies. (E) Improved delivery of Casp-9 via cationic (orange circles) triarginine NG functionalization. (F) Amount of casp-9_{cD} protein delivered is comparable to that of casp-9. (G) Delivery of casp-8 detected using an anticleaved casp-8 antibody. (H) Normalized intensity (caspase small subunit intensity/loading control intensity) of the various caspases at 1 mg/mL; error bars correspond to SEM of three independent biological NG batches, made and tested on separate days. One-way ANOVA was performed against casp-3 NG, and no significant (n.s.) differences were found.

6% respectively, Figure 3F). Hence, assessing WT casp-9 and casp-9_{cD} as therapeutic cargos may reveal different apoptotic outcomes and mechanisms upon initiator caspase delivery. While it is clear that executioners casp-6 and -7 are protected by NG formation, initiators casp-8 and -9 appear not to be when assayed against peptide substrates that interact only with the active site.

All NG-Released Apoptotic Caspases Demonstrate Substrate Proteolysis in Lysates

Because caspases are known to rely on allosteric interactions,[58] exosites,[59,60] and other molecules to stimulate substrate recognition and recruitment, it is critical that we evaluate NG-released caspase activity with native substrates, in addition to the synthetic peptides assessed above. To assess NG-released caspase activity toward protein substrates in a biological context, casp-NGs were kept intact or disassembled with DTT prior to incubation with cell lysates (workflow in Figure S3). Consistent with casp-3 NG-mediated cell death previously reported,[10,61] NG-released casp-3 demonstrated cleavage of known apoptotic substrates including poly(ADP-ribose) polymerase 1 (PARP-1),[45,62] full-length casp-6,[51] and cochaperone p23[45] in three different cell lines (Figure 3G). NG-released casp-6 demonstrated processing of known substrates including segment polarity protein disheveled homologue (DVL3),[60] α-tubulin,[63] lamin A,[60,64] and Parkinson's Disease protein 7 (PARK7 or DJ-1)[60] (Figure 3H). NG-released casp-7 demonstrated cleavage of known substrates PARP-1, full-length casp-3,[64] and p23[45] (Figure 3I). Notable substrate cleavage was observed in the absence of exogeneous DTT for some NGs, i.e., PARP-1 cleavage by casp-7 NG ± DTT (Figure 3I). We hypothesize that this cleavage, in the absence of DTT, is due to casp-NG disassembly and protein release by endogenous glutathione in cell lysates. Thus, all of the NG-released executioner caspases are robustly capable of cleaving native protein substrates in the cytoplasm.

The initiator caspases can also be functionally released from the NG. NG-released casp-8 induced cleavage of known caspase-8 substrate BH3 interacting domain death agonist (BID)[3,42] to tBID (truncated BID) in all three cell lysates tested (Figure 3J). These data suggest that despite minimal peptidyl substrate turnover by NG-released casp-8 (Figure 3D), initiator casp-8 is capable of substrate proteolysis upon delivery. In fact, casp-8's activity might be expected to increase within the biological context due to a shift to a predominately dimeric state, although likely not via recruitment to the DISC, which requires extracellular factors and DED domain interactions. Further, NG-released casp-8 demonstrated processing of PARP-1 to an 89 kDa fragment at the site recognized by casp-3 or -7 but not at the site cleaved by casp-8 which results in a 48 kDa fragement[65] (Figure 3K). This observation suggests that NG-released casp-8 activated executioner procasp-3 or -7, which then cleaved PARP-1. PARP-1 is a predominate substrate of casp-7 and a minor substrate of casp-3, with cleavage rates of 20 and 0.4 ($\times 10^5$ M^{-1} s^{-1}), respectively.[66] Accordingly, procasp-3 activation by casp-8[41] was visualized over time in HEK293T cells. This was similar to the results for NG-released casp-6 (Figure 3L), which we attribute to NG-released active casp-6 mediating a feedback loop, activating procasp-8.[38] Casp-9 and casp-9_{cD} NGs also induced PARP-1 cleavage in two cell lines (Figure 3M), mirroring the enhanced cleavage induced by casp-9_{cD} that was observed for peptidyl substrates (Figure 3E vs 3F). These data suggest that even though NG-released initiator caspases

https://doi.org/10.1021/jacsau.1c00261
JACS Au 2021, 1, 1240–1256

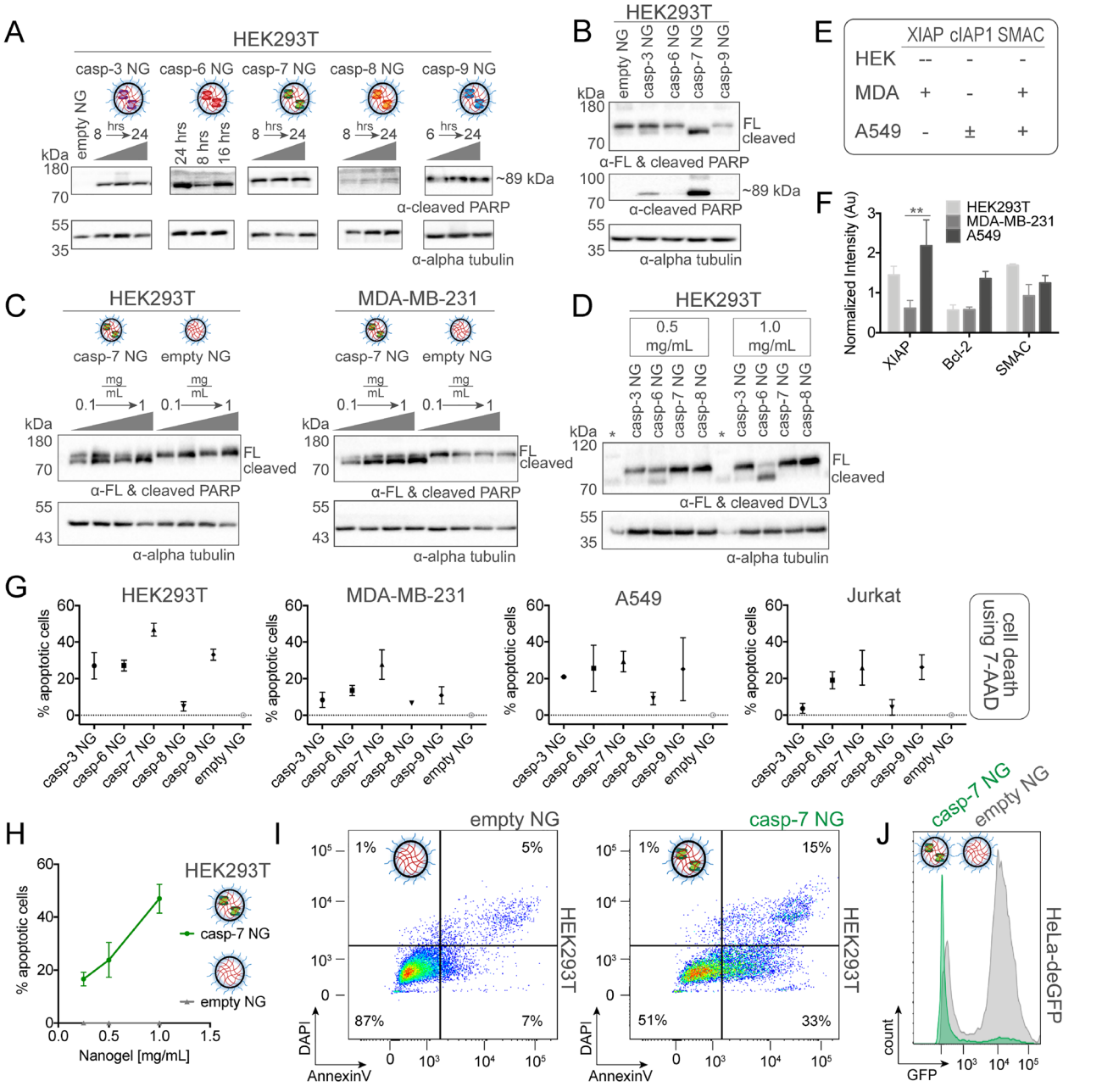

Figure 5. Casp-NG mediated cleavage of PARP-1 and DVL3 and cell death profiles. Immunoblot analysis of NG-treated cell lysates and resultant poly(ADP-ribose) polymerase 1 cleavage over time. (A) Casp-3, casp-6, casp-7, and casp-9 NG induced PARP-1 cleavage in HEK293T cells. Time course experiments were executed once for each casp-NG. (B) In a direct comparison, PARP-1 is cleaved most abundantly by casp-7 NG followed by casp-3 NG in HEK293T cells. Full-length PARP-1~115 kDa, cleaved ~89 kDa. (C) PARP is cleaved in a dose-dependent manner by casp-7 NG in HEK293T and MDA-MB-231 cells. Casp-NG induced PARP-1 cleavage experiments were executed in two biological replicates, with different NGs made and tested on different days. (D) Segment polarity protein disheveled homologue is cleaved in a dose-dependent manner mostly by casp-6 NG in HEK293T cells in two biological replicates; *indicates visible molecular weight marker. (E) Previously reported levels of pro-survival proteins: IAP levels in HEK293T cells,[68] IAP levels in MDA-MB-231 and A549 cells,[69] and SMAC levels in all three cell lines.[70] Labels depict protein levels related to the calculated average (±): lower (−) or higher (+). (F) Quantification of pro-survival protein levels in respective cell lines, normalized to α-tubulin loading control. Two-way ANOVA preformed for significance test. Casp-NG induced varying levels of cell death in all cell lines, with casp-7 emerging as the most potent apoptotic cargo. (G) Relative casp-NG (1 mg/mL) cell death profiles were monitored in HEK293T, Jurkat, MDA-MB-231, and A549 cells, measured using 7-AAD and normalized to empty NG controls. (H) Casp-7 NG induced apoptosis in a dose-dependent manner. All error bars correspond to SEM of two independent NG batches, made and tested on separate days. (I) Casp-7 NG induced a significant population of early apoptotic (33 vs 7% empty NG) and late apoptotic/dead cells (15 vs 5%) measured with AnnexinV and DAPI. AnnexinV experiments were biologically replicated, but data herein represent one biological replicate. (J) Casp-7 NG significantly depletes GFP signal in HeLa-GFP cells, indicating ample cell death. Data herein represent one biological replicate.

demonstrated low peptide substrate turnover in a test tube, NG formation did not silence initiator caspase activity. Moreover, as these proteases are known to require additional protein complexes for maximum substrate turnover, total cell lysate proteolysis assays represent the full potential of NG-released proteolytic activity within the cellular environment. These data

https://doi.org/10.1021/jacsau.1c00261
JACS Au 2021, 1, 1240−1256

Scheme 2. (A) Presumed Routes to Apoptosis upon Exogenous Introduction of Active Apoptotic Caspases[a] and (B) Levels of Pro-survival Factors That Regulate Caspases and Apoptosis, Such as XIAP,[68] cIAP1,[69] and Bcl-2,[78] Vary Depending on Cancer Type and Are Correlated with Clinical Chemotherapeutic Outcomes[b]

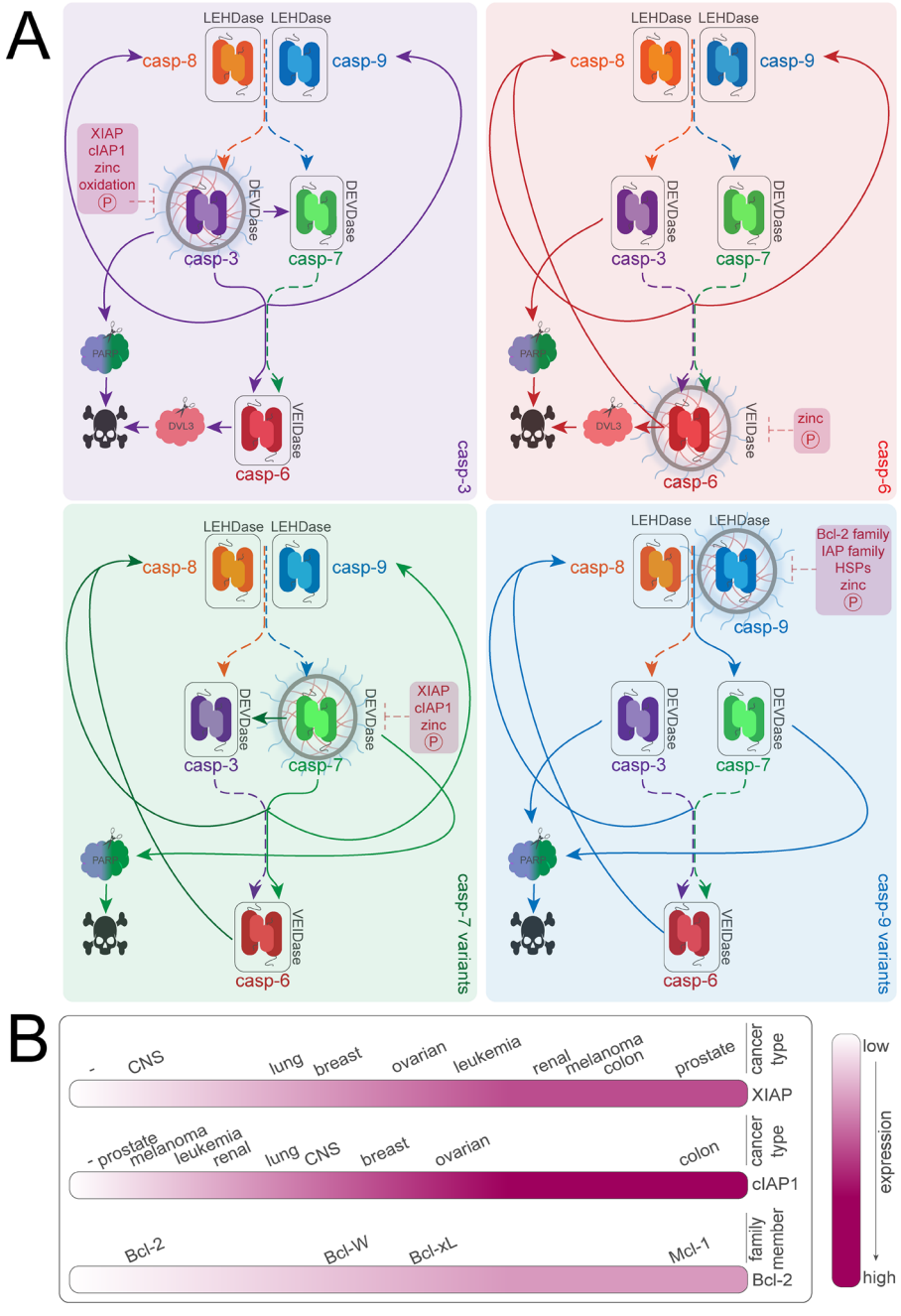

[a]Introduced caspases (NG symbol) promote varying degrees of known apoptotic hallmarks (Scheme S1).[33−43,41−43] These measured outcomes include cleavage of substrates (PARP-1, DVL3) and activity of both initiator (LEHDase) and executioner (VIEDase, DEVDase) caspases (Table S3). Knowledge of these differences combined with known differences in inhibition by modifications and pro-survival factors (pink box) leads to these presumed routes. [b]This provided a rationale for observed differences in apoptotic propensity between different endogenously introduced caspases.

convincingly demonstrate that both executioner and initiator caspases can be released in a functional manner in the cytosol and can cleave their native apoptotic substrates.

All Apoptotic Caspases Are Exogenously Introduced at Comparable Protein Levels

Given that caspases are released in a functional manner in cell lysates, we next assessed NG-mediated caspase delivery to intact cells in culture. We first evaluated delivery by fluorescently (Cy5) tagging full-length, active-site-knockout caspases prior to NG formation. The active-site knockouts were used so that caspase-induced apoptosis did not confound evaluation of casp-NG cellular uptake. Flow cytometry revealed that all caspases were delivered in a similar dose-dependent manner (Figure S4). To further visualize delivery in a fluorescence-independent assay, we immunoblotted for the delivered caspases monitored by their His_6-tags. In HEK cells, we visualized internalization of

https://doi.org/10.1021/jacsau.1c00261
JACS Au 2021, 1, 1240−1256

active casp-3 after 8 h at two different doses (Figure 4A). Delivered active casp-6, casp-7, casp-9, and casp-9_{cD} were observed at similar levels (Figure 4B−D,F). We have previously reported that functionalization of casp-3 NG with a triarginine peptide (R^3) resulted in an increase in the total amount of protein delivered.[10,61] Here, we likewise observed that upon R^3 addition to casp-9 NGs, the delivery efficiency of casp-9 increased (Figure 4E). Casp-8 delivery was also observed in multiple cell lines in a dose-dependent manner (Figure 4G and Figure S5), but due to the failure of casp-8 detection using the His_6 antibody, we used a highly specific casp-8 antibody. Delivery of all caspases fell within a 2-fold range and is not statistically significantly different (Figure 4H), strongly supporting our conclusion that delivery is independent of the identity of the caspase cargo.

Exogenously Introduced Casp-7 Emerges as Most Effective Apoptosis-Inducing Cargo

Upon confirming that detectable levels of protein were delivered, we then assessed various apoptotic markers upon delivery of the different caspases in cells. Cells undergoing apoptosis display a multitude of time-dependent morphological and biochemical changes such as cell shrinkage, loss of plasma membrane integrity, and PARP-1 cleavage[62] to indicate faulty DNA repair during chromatin degradation, facilitating nuclear disintegration.[67] We observed significant cleavage of PARP-1 by casp-3, -6, -7, and -9 NGs but not casp-8 NG within 8 h (Figure 5A). However, in a direct comparison, the amount of PARP-1 cleaved by casp-7 NG overshadowed the amount cleaved by the other caspases (Figure 5B). PARP-1 cleavage induced by casp-7 NG was observed in a dose-dependent manner in two cell lines (Figure 5C). As PARP-1 is a substrate of casp-3 and -7,[45] casp-3 or -7 NG facilitated rapid cleavage of the delivered cargo's direct substrate (Scheme S1 and Scheme 2). On the other hand, casp-6 or -9 NG may induce indirect cleavage of PARP-1 via different mechanisms: delivered casp-9 may directly activate procasp-3 or -7,[35,39,40] while casp-6 may activate procaspase-3 directly[44,46] or procaspase-8,[38,35] thus leading to casp-3 and -7 activation (Scheme S1 and Scheme 2). Additionally, cleavage of the casp-6 substrate DVL3[60] was most significant with casp-6 NG but was also observed with casp-3 NG (Figure 5D). These data demonstrate specific substrate turnover by executioner casp-3, -6, and -7 in cellulo upon NG delivery.

We anticipated that caspase activity (e.g., PARP-1 cleavage) in cells should correlate with the ability of delivered caspases to induce cell death. Importantly, to understand the role of the cellular apoptotic balance in cell death mediated by caspase-NGs, we evaluated casp-NG-mediated cell death in cell lines with different pro-survival and pro-apoptotic protein equilibria (Scheme 2B). Specifically, protein levels of two IAPs, X-linked (XIAP) and cellular (cIAP1), varied in the literature across HEK293T (kidney), MDA-MB-231 (breast cancer), and A549 (lung cancer) cells (Figure 5E).[68−71] XIAP is known to bind and inhibit casp-3, -7, and -9 distinctly (Table S2).[72,73] Yet, cIAP1 has been characterized to bind, but not inhibit, casp-3, -7,[74] and -9,[75] while also influencing casp-8's ability to propagate apoptosis.[76] We quantified levels of XIAP, along with its pro-apoptotic antagonist second mitochondrial activating factor (SMAC/Diablo)[70,77] and pro-survival protein Bcl-2[78] in our cell lines (Figure 5F) and observed that the levels differed slightly from those reported.[68−71] This underscores the importance of assessing cell death in different cell lines, as well as examining the protein levels in the exact cells being used, to allow meaningful correlations with observed outcomes. Notably, we also tested Jurkat T-lymphocytes, a leukemic representative suspension cell line, where elevated IAP levels are reported to hinder leukemic therapies.[69]

Casp-NG induced apoptosis was measured using 7-amino-actinomycin D (7-AAD) (Figure S6).[79,80] In HEK293T cells, the amount of apoptosis induced by casp-6 and casp-9 NGs was similar to that of casp-3 NG (Figure 5G). As predicted by the extensive PARP-1 cleavage induced by casp-7 NG (Figure 5A−C), casp-7 NG induced the most cell death of all casp-NGs (Figure 5G). Similarly, consistent with the lack of activity and substrate cleavage observed by casp-8 NG, this nanomaterial failed to induce noticeable apoptosis compared to empty NG controls (Figure 5G). Thus, we observed some correlation between substrate cleavage and induced cell death in HEK293T cells, which are reported to have the lowest protein levels of IAPs (Figure 5E,F) and, thus, were the most susceptible to cell death. In contrast, the cell death profiles observed for casp-3, -7, and -9 appeared to reflect a different cellular apopototic context, with casp-7 NG inducing the most apoptosis overall. MDA-MB-231 cells are reported to have higher levels of XIAP (Figure 5E,F), and delivery of casp-3, -7, and -9 was less efficient at inducing apoptotic cell death than in other cell lines (Figure 5G). On the other hand, casp-6 is not inhibited by XIAP but is also less efficacious at inducing apoptosis in MDA-MB-231 cells, suggesting that other apoptotic regulators may also be in play. Together, these data support the idea that the levels of anti-apoptotic factors, particularly XIAP, present in a given cell type have an ability to modulate caspase-induced cell death.

Delivered casp-7 and casp-9_{cD} were the most effictive at inducing apoptosis. Casp-7-NG-mediated apoptosis was observed by 7-AAD in a dose-dependent manner (Figure 5H) and by AnnexinV staining of 48% of cells (Figure 5I). Consistent with the increased catalytic activity of casp-9_{cD}, ∼2-fold more apoptosis and 79% AnnexinV positive cells were observed upon casp-9_{cD} NG treatment relative to casp-9 NG (Figure S7). Finally, casp-7 NG treatment of cells stably expressing GFP (i.e., HeLa expressing destabilized GFP, HeLa-deGFP[81]) significantly decreased GFP signal (Figure 5J), suggesting efficient induction of apopototic cell death.[82] A redox-controlled casp-7 (casp-7_{HC})[83] also effectively induced PARP-1 cleavage and cell death upon exogenous introduction (Figure S8). Together, these data demonstrate that the different apoptotic caspases, including those with intrinsically slower rates of proteolysis than casp-3, can be effectively delivered to induce apoptosis. We hypothesize that their efficacy could be due to the cooperation of unique mechanisms including the ability of each caspase to tolerate NG formation, the significance of substrates cleaved, the repertoire of anti-apoptotic factors expressed that impact each caspase, as well as feedback for activation of other procaspases.

Activation of Native Caspases Dictates Casp-NG Efficacy for Inducing Apoptosis

A number of activation and regulation feedback loops have been reported between the different caspases and their pro-survival partners,[33−43] spurring us to examine the mechanisms contributing to the data observed. For example, casp-7 NG clearly demonstrated extensive cleavage of PARP-1 (Figure 5A−C) and cell death (Figure 5G). These data beg the question as to why exogenously delivered casp-7 is more potent than casp-3, which shows greater intrinsic catalytic activity (Table S1). To elucidate mechanistic insights surrounding these findings, we tested two hypotheses. The first, that the delivered enzymes may

https://doi.org/10.1021/jacsau.1c00261
JACS Au 2021, 1, 1240−1256

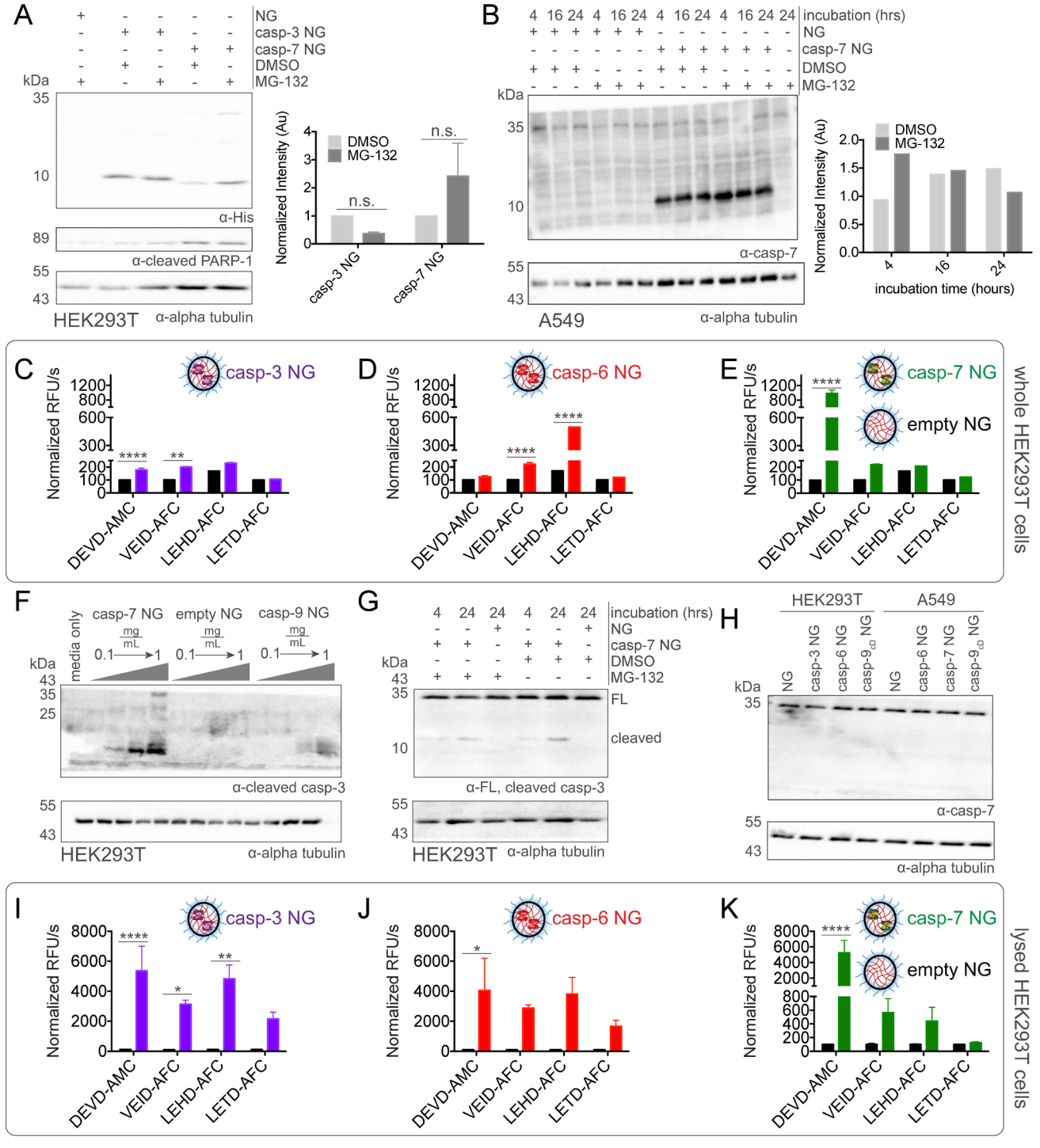

Figure 6. Executioner casp-NG proteolytic profiles after uptake and delivery. (A) Levels of delivered casp-3 and casp-7 do not appear to significantly change in the absence or presence of proteasome inhibitor MG-132 after 24 h incubation in HEK293T cells. Error bars pertain to three independent biological replicates. (B) Levels of casp-7 remain consistent, in the absence or presence of a proteasome inhibitor, from 4 to 24 h in A549 cells in a single biological replicate. Proteolytic profiles of executioner casp-NG after uptake in whole HEK293T cells; resultant amc/afc fluorescence after treatment with (C) casp-3 NG, (D) casp-6 NG, and (E) casp-7 NG. (F) Casp-7 NG treatment results in dose-dependent cleavage of endogenous procaspase-3 in HEK293T cells. (G) Casp-7 NG-induced procaspase-3 cleavage can be observed as a function of time, in the presence or absence of MG-132. (H) Treatment of casp-3, casp-6, and casp-9_{cD} NGs does not demonstrate significant procaspase-7 activation. Proteolytic profiles of executioner casp-NG after uptake in lysed HEK293T cells; resultant amc/afc fluorescence after treatment with (I) casp-3 NG, (J) casp-6 NG, and (K) casp-7 NG. All error bars correspond to SEM of two independent NG batches, made and tested on separate days.

be degraded upon delivery at distinct rates. The second, that the delivered caspases are functioning uniquely within the endogenous caspase pathway; i.e., the less apoptotic cargos are functioning as single proteases, whereas the more apoptotic casp-7 cargo may be activiating endogenous caspases. Beginning with our first hypothesis, we assessed delivered casp-3 and casp-7 levels (after casp-NG treatment) in the presence or absence of proteasome inhibitor MG-132.[84,85] We observed no statistically

https://doi.org/10.1021/jacsau.1c00261
JACS Au 2021, 1, 1240−1256

significant proteasomal degradation of delivered casp-3 or casp-7, as assessed by MG-132-based inhibition of the proteasome (Figure 6A). To more robustly address the influence of MG-132 on casp-7, we directly monitored cleaved casp-7 levels in A549 cells over time and, again, observed no evidence of significant proteasomal degradation (Figure 6B). These data suggest that casp-3 and casp-7 are not degraded by the proteasome at statistically different rates upon exogenous introduction.

Next, to assess which caspases have been activated, after casp-NG treatment, cells were harvested and then subjected to incubation with fluorogenic peptide substrates (workflow in Figure S9). The fluorogenic peptide substrates used include DEVD-amc (casp-3/-7), VEID-afc (casp-6), LEHD-afc (casp-8 and -9), and LETD-afc (casp-8).[86] Cleavage of peptide substrates could be clearly observed after NG treatment. Casp-3/-7 substrate DEVD-amc was cleaved approximately 2-fold above baseline levels upon treatment with casp-3 NG (Figure 6C). However, a similar level of fluorescence was also visualized for VEID and LEHD substrates after casp-3 NG treatment, indicating that casp-3 activated some endogeneous procasp-6 and procasp-8/-9 (Table S3 and Scheme 2). Casp-6 NG treatment also demonstrated a 2-fold increase in proteolytic activity toward casp-6 substrate VEID (Figure 6D), consistent with casp-6 NG-induced cleavage of DVL3 (Figure 5D).[60] More significantly, casp-6 NG demonstrated a 5-fold increase in activity of casp-8/9 substrate LEHD, suggesting that casp-6 activated procaspase-8 and/or -9 (Table S3 and Scheme 2). Due to the known activation of casp-8 by casp-6,[32] we hypothesize that casp-8 is most likely responsible for the observed LEHDase activity. Lastly, casp-7 NG treatment demonstrated a 10-fold increase in intracellular activity toward DEVD-amc (Figure 6E). This activity is the result of the exogeneously delivered casp, but also may reflect the activity of endogeneous procasp-3 and/or -7 that has been activated by delivered casp-7. Although it is impossible to detect endogenously cleaved casp-7 upon recombinant casp-7 delivery, we were able to observe dose-dependent cleavage of endogenous casp-3 (Figure 6F), in the presence or absence of MG-132, a proteasome inhbitor (Figure 6G). These data clearly indicate that the significant DEVD-amc proteolysis observed upon casp-7 NG treatment (Figure 6E) is representative of caspase feedback loops activating endogenous procasp-3. On the other hand, and in accordance with the lower levels of DEVD-amc proteolysis observed by casp-3 NG (Figure 6C), casp-3 NG did not result in noticeable cleavage of endogeneous procaspase-7 (Figure 6H). Overall, the observed activation of caspases appears to be in line with known caspase activation pathways (Scheme S1) and correlates well with the observed levels of cell death (Figure 5G).

While levels of cell death correlated with caspase activities, we sought to determine whether caspases were fully released or whether both activities could be increased by additional caspase release in the cytosol. As our NGs are redox-responsive, we typically assessed caspase activity in the absence of added reductant to ensure that the activity evaluated is from cytosolically disassembled casp-NG. Nevertheless, additional reductant would (i) maximize caspase activity by ensuring reduction of the caspases's catalytic cysteine residue and (ii) may also elucidate if casp-NG have reached the cytosol but fail to disassemble/release the protein. Upon the addition of 0.5 mM DTT, we observed higher levels of fluorogenic peptide proteolysis for casp-3-NG-treated cell lysates toward DEVD substrate, casp-6-NG toward DEVD/VEID/LEHD/LETD substrates, and casp-7 toward DEVD/VEID/LEHD substrates (Figure S10). Interestingly, casp-3 NG (7-fold) and casp-6 NG (11-fold) were activated more by the addition of reductant than was casp-7 NG (3.5-fold), indicating a difference in redox sensitivity for the cargos that could correspond to factors such as active site oxidation or release from the NG. Casp-7 has been observed to influence reactive oxygen species production and accumulation during apoptosis, whereas casp-3 does not, underlying a distinct redox difference between the two DEVDases.[40] These data unambiguously indicate that proteolysis and procaspase activation by the various caspase cargos is directly related to, and could be further improved upon, delivery vehicle and release compatibility optimization. In summary, we hypothesize that the phenomenon of casp-7 outperforming casp-3 may be unique to redox-responsive materials, and carefully investigating different caspase cargos within different delivery systems (redox-responsive and nonredox-responsive) may be an informative future investigation.

Low levels of endosomal escape routinely hinder delivery efficacy.[87,88] Thus, we hypothesized that if casp-NGs are largely trapped in endosomes, upon cell lysis, significantly more caspase activity should be observed. To test this hypothesis, we measured proteolytic activity in lysed cells (workflow Figure S9). When endosomes were disrupted, dramatically more activity toward multiple substrates was observed upon cell lysis for all executioner NGs. Casp-3 and casp-6 NGs both induced ≥20-fold activity toward all four substrates, indicating that if more casp-3 and -6 NGs escaped the endosome, the caspase cargos would be appreciably more powerful in activating endogenous procaspases (Figure 6I,J). On the other hand, lysed casp-7 NG-treated cells increased cleavage of DEVD-amc 60-fold, whereas VEID-afc and LEHD-afc only increased 4-fold (Figure 6K). Thus, unlike casp-3 and casp-6, which activate initiator caspases, casp-7-mediated cell death appears to be due to exogeneous casp-7 activity itself or combined with activation of executioners procasps-3 and -7 (Scheme 2). In comparing exogenously delivered casp-3 and casp-7, the differences in the initial rate of DEVD-amc cleavage (Figure S11) reflect the intrinsic differences in catalytic efficiency between the two enzymes (ST 1). Casp-3 NG achieved maximum substrate turnover within 4 h, whereas casp-7 NG continues to increase over several days, consistent with the distinct enzymatic efficiencies of the two DEVDases.[56] These data suggest that there is merit for further investigations of the different apoptotic cargos as there may be differences in apoptotic time scales and the background of apoptosis inhibitors in various cells which could result in more tunable therapeutics. Moreover, these data demonstrated that if more endosomal escape is achieved, the executioner casp-NG can clearly feedback more effectively to propagate caspase activation.

CONCLUSIONS AND OUTLOOK

Cancers from different organs and disease stages are known to overexpress pro-survival proteins to different extents.[69,89−91] This finding underscores the need for personalized medicine, which recognizes the central importance of tailoring a specific therapy to individual disease variants. Pro-apoptotic proteins, such as caspases, offer the opportunity to exogenously overcome unique apoptosis desensitization phenotypes in various cancers. Being a native cellular component, caspases have the advantage of being active only in their targeted microenvironment, thus providing inherent selectivity. However, prior to this work, which initiator or executioner caspases would be most effective in inducing apoptosis when introduced exogenously remained

https://doi.org/10.1021/jacsau.1c00261
JACS Au 2021, 1, 1240−1256

completely unknown. A number of prior reports underscore the fact that each caspase is uniquely regulated and is subject to inactivation by different factors.[74,78,92−95] Furthermore, various cell lines (our somewhat simplistic proxy for different disease variants in this study) display different levels of caspase inhibitors and other anti-apoptotic (proliferative) elements (Scheme 2). These two factors together suggest that various cell lines with their unique suite of overexpressed anti-apoptotic factors (Figure 5E,F) might be differentially susceptible to the induction of apoptosis.

To explore that hypothesis, casp-3, -6, -7, -8, and -9 were successfully encapsulated within nanogels and were delivered intracellularly, demonstrating varying levels of proteolysis in vitro and in cellulo (Table S3). We hypothesize that uptake and endosomal escape are dominated by the properties of the polymer used for encapsulation and delivery. Because the same polymer was used to deliver all caspases, differences in apoptotic efficacy should be attributed to (i) the effect of NG formation on enzymatic activity and function, (ii) the inherent catalytic properties of each caspase in the cytosol at the resultant concentration, and (iii) the environment various caspases encounter in different cell lines or subcellular locations. Formation of these NGs was straightforward and reproducible. Thus, we envision that the required polymeric components could be packaged and distributed for widespread use within the research community for exogenous introduction of many cysteine-containing protein cargos.

It is critical to note that while all caspases were effectively encapsulated and delivered in an active form, not all caspases showed the same propensity to induce cell death. Casp-7 and casp-9_{cD} stood out as the most potent apoptosis inducers in several assays, showing even greater apoptosis-inducing potential than that with casp-3 (Table S3). Casp-3 is the family member with the highest enzymatic efficiency,[45,56] widest substrate pool,[7,48,86] and its activation unambiguously correlates with efficient apoptosis in numerous cancer cells upon a myriad of stimuli (e.g., drugs).[34−36,40,44] These data imply that the alterations to pro-survival elements may have been adopted as a forceful strategy to block casp-3 activity, thus making casp-7 and -9 better situated to induce apoptosis in those cells.

The observed difference of casp-3 and -7 to induce cell death was striking given that casp-3 and casp-7 are similar executioner DEVDases. This may also suggest that distinct differences in mechanisms of their inhibition (i.e., phosphorylation[94] or metal binding,[92] Table S2) may impact their death-inducing potential (Scheme 2). Furthermore, as we observed that the addition of exogeneous reductant influenced in cellulo caspase proteolytic activity, it is possible that the findings herein are unique to redox-responsive delivery systems. On the other hand, casp-3 may be more susceptible to oxidation or other cysteine blocking mechanisms than casp-7 (i.e., glutathionylation,[95] Table S2). Echoing the conventional wisdom of the hierarchical caspase pathway, and in agreement with the vast apoptotic literature, we conclude that maximal apoptosis is observed upon caspase feedback loops activating procasp-3 or relieving active casp-3 inhibition.[35,36,44,96] The exogenous introduction of casp-7 demonstrated high levels of apoptosis due to endogenous procaspase-3 activation. Therefore, in cell lines with apoptotic-resistant phenotypes, wherein casp-3 activity is often compromised, targeting casp-7 or points upstream of casp-3 inhibition should be explored as strategies to push diseased cells to die.

The only caspase that failed to induce cell death was casp-8 (Table S3). To take advantage of casp-8's role in the extrinsic apoptotic pathway, delivering full-length casp-8 with the DED domain may better facilitate propagation of apoptosis via the DISC which is not mediated by the DED-deleted casp-8 used herein. Casp-6 NGs induced levels of cell death comparable to those of casp-3, but most importantly, casp-6 induced the most LEHDase activity, suggesting the most procasp-8 and -9 activation in cellulo (Table S3 and Scheme 2). In summary, these data strongly indicate that various caspases, particularly casp-7 and casp-9, effectively induce apoptosis with significant therapeutic potential. Moreover, these results suggest that the use of particular caspases, perhaps complimented with other pro-apoptotic factors, may allow optimal cell killing in various disease states, such as cancers, each with their own unique anti-apoptotic status (Scheme 2).

In the field of delivery, different delivery vehicles are often compared. Yet, comparing distinct cargo, even members of the same family, is often overlooked due to formulation limitations. Here, for the first time, direct comparison of different apoptotic caspases as apoptotic cargos was assessed. Although there may be some influence on the chemistries of the materials used for exogenous introduction, this study demonstrates the clinical potential of caspases other than casp-3 to induce apoptosis. The mechanistic findings herein show that judicious matching of the target cells and the functional cargo enable us to maximize therapeutic efficacy. In future systems, caspases can be combined with chemotherapeutics to maximize endogenous caspase activation or with pro-survival antagonists to relieve diseased interactions or prevent inhibition of the delivered cargo. Moreover, specific caspases and/or combinations may now be tailored to particular tissue types to overcome disease characteristics and shift the equilibrium to favor death.

MATERIALS AND METHODS

Caspase Random Copolymer NG Formation

Procedures for casp-NG formation were followed similarly to those previously described for casp-NG.[10] Twenty mg of random PEG−PDS was added to a vial and dissolved in 1 mL of 1× PBS, pH 7.4, via sonication for a final concentration of 20 mg/mL polymer. This polymer stock solution was stirred at 4 °C for ∼1 h before 0.5 mL was aliquoted into a new vial. To the 10 mg polymer aliquot was added a solution (containing casp-3, casp-6, casp-7, casp-8, or casp-9) at a weight ratio of 25:1 polymer/protein with additional 1× PBS to achieve a final concentration of 10 mg/mL (or a final volume of 1 mL). The polymer−protein solution was left to stir for ∼3 h at 4 °C. The conjugates were then cross-linked with dithiothreitol and additional stirring for ∼1 h at 4 °C. The NG conjugates were then purified via dialysis against 1× PBS, pH 7.4 using a 100k MWCO aqueous membrane for ∼20 h at 4 °C with multiple buffer changes. Dialysis against this large membrane allows removal of the cross-linking byproduct pyridine-2-thiol, DTT, and unencapsulated protein. Prior to dialysis, cross-linking and functionalization were quantified using 2 μL of the NG solution + 98 μL of water ± excess DTT and recording the absorbance of the cross-linking byproduct at 343 nm using UV−vis spectroscopy.

Assessing Activity of NG-Released Caspase Using Fluorogenic Peptide Substrates

For a control to assess loss of caspase activity, during NG formation, the corresponding caspases were diluted to 12 μM and stored in 1× PBS, pH 7.4 at 4 °C for the same amount of time as NG formation + dialysis procedure. After dialysis, two samples of purified casp-NG were diluted in the corresponding caspase activity buffer in the presence of DTT or water to release or maintain entrapment of the encapsulated protein. In the same 96-well plate, the control free protein (stored at 4 °C for ∼24 h) was diluted similarly based on the amount of NG protein in the sample (calculated using NG encapsulation efficiency). After a 10 min

https://doi.org/10.1021/jacsau.1c00261
JACS Au 2021, 1, 1240−1256

incubation, a volume of each reaction was added using a multichannel pipet to wells containing the corresponding substrate in DMSO. The activity in each of the samples was immediately measured in duplicate over a time course at 37 °C as the increase in fluorescence of cleaved coumarin measured in a Spectramax M5 spectrometer (Molecular Devices, excitation 365 nm; emission 495 nm for amc; excitation 380 nm, and emission 510 for afc). The initial velocity, in relative fluorescence units/s (RFU/s), was reported and normalized to the control with unencapsulated protein. The graphs included in Figure 3 correspond to three individual biological replicates performed on three separate days with individual NG batches. Casp-3 activity buffer: 20 mM HEPES pH 7.5, 150 mM NaCl, $CaCl_2$, 10% PEG 400; substrate: *N*-acetyl-Asp-Glu-Val-Asp-7-amino-4-methylcoumarin (DEVD-amc, Enzo Life Sciences). Casp-3 assay conditions: 50 μL of reaction mixture added to 5 μL of 0.5 μM substrate. Casp-6 activity buffer: 100 mM HEPES, pH 7.5, 100 mM NaCl, 10% sucrose, 0.1% CHAPS; substrate: *N*-acetyl-Val-Glu-Ile-Asp-7-amino-4-methylcoumarin (VEID-afc, Enzo Life Sciences). Casp-6 assay conditions: 50 μL of reaction mixture added to 5 μL of 0.5 μM substrate. Casp-7 activity buffer: 100 mM HEPES, pH 7.5, 5 mM $CaCl_2$, 10%, PEG 400, 0.1% CHAPS, substrate: *N*-acetyl-Asp-Glu-Val-Asp-7-amino-4-methylcoumarin (DEVD-amc, Enzo Life Sciences). Casp-7 assay conditions: 50 μL of reaction mixture added to 5 μL of 0.5 μM substrate. Casp-8 activity buffer: 10 mM PIPES, pH 7.2, 100 mM NaCl, 1 mM EDTA, 0.05% CHAPS, 10% sucrose; substrate: *N*-acetyl-Leu-Glu-His-Asp-7-amino-4-methylcoumarin (LEHD-afc, Enzo Life Sciences, LETD-afc, was also tested). Casp-8 assay conditions: 50 μL of reaction mixture added to 10 μL of 0.5 μM substrate. Casp-9 activity buffer: 100 mM MES, pH 6.5, 10% PEG 8000; substrate: *N*-acetyl-Leu-Glu-His-Asp-7-amino-4-methylcoumarin (LEHD-afc, Enzo Life Sciences). Casp-9 assay conditions: 100 μL of reaction mixture added to 10 μL of 0.5 μM substrate.

Immunoblotting

Lysates were assayed for the total protein concentration using the bicinchoninic acid assay (Pierce). Lysates were diluted to attain identical protein concentrations in each sample, and SDS-PAGE samples were immediately diluted into denaturing, reducing sample buffer and heated to 95 °C for ∼10 min. Twenty μL of lysate samples were loaded into a 16% SDS-PAGE, and electrophoresis was executed at 175 V for 70 min. Samples were then transferred to a PVDF membrane (Millipore) at 100 V for 140 min, with two ice block changes. After transfer, membranes were blocked using OneBlock Western-CL blocking buffer (Genesee Scientific) for 60 min at room temperature and then cut into appropriate molecular weight ranges to probe for specific proteins. Membranes were incubated with the primary antibody overnight at 4°C with constant rotation. Primary antibodies, purchased from Cell-Signaling Technologies, were used at a 1:1000 dilution including anti-α-tubulin (#2144S), anti-His (#12698S), anti-cleaved casp-8 (#9748S), anti-PARP (#9532S), anti-cleaved PARP (#9541S), anti-casp-3 (#9662S), anti-casp-6 (#9762S), anti-casp-7 (#9492S), anti-DVL3 (#3218S), anti-DJ-1 (#2134S), anti-XIAP (#14334S), and anti-cleaved lamin A (#2035S). Primary antibodies purchased from Santa Cruz Biotechnology were used at a 1:200−1000 dilution including anti-Bcl-2 (SC-7382), anti-BID (SC-373939), and anti-p23 (SC-101496). Finally, a SMAC/Diablo antibody was purchased from Novus Biologicals (#56311SS) and was used at a 1:250 dilution. Membranes were then washed with 1× TBST three times for 10 min each and then probed with a secondary goat anti-rabbit HRP antibody (#20-303, Genesee Scientific) or goat anti-mouse HRP antibody (Jackson AffiniPure115-035-003) at 1:20,000 dilution for 1 h at room temperature. Membranes were then washed again with 1× TBST three times for 10 min each followed by incubation with SuperSignal West Duration substrate (#34075, Thermo Fisher) for 2−3 min at room temperature and imaged using the ChemiDoc MP imaging system (BioRad). Blots were quantified using ImageJ and normalized to the α-tubulin loading control.

NG-Released Caspase Activity toward Protein Substrates in Lysate

To a solution of purified casp-NG (100 μL, 7 mg/mL), 20 μL of 1 M DTT or water was added to release or maintain entrapment of the encapsulated protein. After a 10 min incubation, 30 μL of these solutions were added to 60 μL of homogeneous cell lysate (HEK, Jurkat, or MDA-MB-231) and 20 μL of the corresponding caspase activity assay buffer. The zero time point was immediately taken by removing 30 μL of this solution and mixing it with 10 μL of SDS-PAGE 3× dye (with reductant) and immediately heated at 95 °C for ∼5 min. The remaining reaction was left to incubate at 37 °C for several hours. After incubation, the final time point was taken identically and samples were assayed by Western Blot.

Adherent Mammalian Cell Studies for Delivery Evaluation by Western Blot

Briefly, all adherent cells were grown in 100 mm × 15 mm tissue culture dishes in the presence of DMEM (Gibco, Thermo Fisher) supplemented with 10% FBS (Gibco, Thermofisher) and 1% penicillin/streptomycin (Gibco, Thermo Fisher) at 37 °C, 5% CO_2 until ready for use. Two days prior to cellular assessment, cells were plated at a density of $\sim 5 \times 10^4$ in a 24-well plate and left to adhere for ∼24 h. The day before the assay, purified NG samples were diluted in the appropriate cell culture media with 10% 1× PBS. Plates were then left to incubate. After incubation, cells were washed twice with 1× PBS (Gibco, Thermo Fisher) and then lysed with 60 μL of freshly prepared and sterile filtered lysis buffer. Lysis buffer contained 50 mM Tris, pH 8.0, 150 mM NaCl, 1% Triton-X 100 and 10 mM DTT with 1× halt protease/phosphatase inhibitor cocktail (Pierce, Thermo Fisher). Culture plates were incubated at 4°C for 25 min with constant rotation. Lysates were then extracted and clarified by centrifugation for 20 min at 16,000*g*, 4°C.

Suspension Mammalian Cell Studies for Delivery Evaluation by Immunoblot

Briefly, Jurkat cell suspensions were cultured in T75 flasks in RPMI 1640 media (Genesee Scientific) supplemented with 10% FBS (Gibco, Thermo Fisher) and 1% penicillin/streptomycin (Gibco, Thermofisher) at 37 °C, 5% CO_2. The day prior to cellular assessment, cells were plated at a density of $\sim 1 \times 10^5$ in a 24-well plate in the presence of PBS containing NG samples, composing 10% of the final solution volume. Plates were then left to incubate. After incubation, the cell suspensions were harvested by centrifugation at 4000*g* for 5 min. Medium was carefully decanted, and cells were lysed on ice by incubation with 60 μL of freshly prepared and sterile filtered lysis buffer. Lysis buffer contained 50 mM Tris, pH 8.0, 150 mM NaCl, 1% Triton-X 100, and 10 mM DTT with 1× halt protease/phosphatase inhibitor cocktail (Pierce, Thermofisher). Lysates were then clarified by centrifugation for 20 min at 16,000*g*, 4°C.

Apoptosis Evaluation Using Flow Cytometry and 7-Aminoactinomycin D

7-AAD can be utilized to distinguish viable, apoptotic, and late apoptotic/dead cells using flow cytometry.[79,80] For adherent cells, after incubation of NG-cell culture 24-well plates, the medium containing detached cells was aspirated and placed in a tube. The remaining adhered cells were not further washed in an effort to save any remaining loosely detached (apoptotic) cells. One hundred μL of 1× trypsin (Sigma) was then added and left to incubate for ∼5 min at 37 °C in 5% CO_2 until all cells were visibly removed from the plate. The 100 μL trypsin/cell solution was removed and added to tubes containing the corresponding aspirated medium. The tubes were then centrifuged at 4000*g* for 5 min to pellet all cells. The supernatant was removed, carefully leaving the cell pellet intact. Two hundred microliters of FACS buffer (sterile filtered 0.5% BSA (#9048-46-8) in 1× PBS, pH 7.4) prepared with 10 μg/mL fresh 7-aminoactinomycin D (7-AAD) was added, and the pellet was gently redispersed via pipetting. Samples were immediately assayed by flow cytometry using a 640 nm laser line. For analysis, cells were gated for live vs apoptotic vs late apoptotic/dead populations (FSC-A vs 7-AAD-A).[79] For suspension cells, when time

https://doi.org/10.1021/jacsau.1c00261
JACS Au 2021, 1, 1240−1256

elapsed for NG cell culture incubation within 24-well plates, the cell suspension was harvested by centrifugation at 4000*g* for 5 min to pellet all cells. Then, an identical procedure to that for adherent cells was followed.

Apoptosis Evaluation Using AnnexinV

AnnexinV staining is routinely used to measure phosphatidylserine exposure, which occurs during apoptosis.[97] Adherent and suspension cells were harvested identically to the flow cytometry procedures described above. The cell pellets were redispersed and supplementary washed twice in 500 μL of a 1× AnnexinV binding buffer (10× buffer: 0.1 M HEPES (pH 7.4), 1.4 M NaCl, 25 mM $CaCl_2$). After washings, the pellets were redispersed in 100 μL in the same buffer, prepared with Cy5-AnnexinV (BD Pharmingen) and NucBlue stain ReadyProbe (Thermo) according to the manufacturer's protocols. After binding, the cells were harvested again and washed twice prior to flow cytometry analysis.

Casp-NG Treatment in the Presence of Proteasome Inhibitor MG-132

Adherent cells were seeded as previously described. When cells reached confluency, cells were treated with 5 μM MG-132 or the appropriate amount of DMSO for 5 h. After incubation, the medium was removed, cells were washed with PBS, and medium was replaced with the NGs present. NGs were left to incubate as previously described and then prepared as lysates for immunoblot analysis.

In Cellulo Assessment of Endosomally Escaped Casp-NG Activity Using Fluorogenic Peptide Substrates

Adherent and suspension cells were harvested identically to the flow cytometry procedures described above, in which cells were cultured in 6-well plates. After pelleting all cells, cells were washed twice via redispersion in 500 μL of a buffer composed of 20 mM HEPES (pH 7.5), 10% glycerol, 0.5 mM EDTA, followed by centrifugation. After two washes, the cell pellets were redispersed in 2250 μL of FACS buffer. This reaction was then aliquoted (500 μL each for four substrates) in the presence of 20 μM of one fluorogenic caspase substrate (see Supporting Information for details related to DEVD-amc, VEID-afc, LETD-afc, IETD-afc, or LEHD-afc). Technical replicates (200 μL each) were plated in tissue culture treated 96-well plates (with top) and left to incubate at 37 °C, 5% CO_2, by reading the plate over time. To prevent evaporation, 100 μL of PBS was added to the surrounding wells.

In Cellulo Assessment of Uptaken Casp-NG Activity Using Fluorogenic Peptide Substrates (Cells Lysed after Treatment)

For fluorogenic peptide substrate analysis of NG-treated lysates, cells were grown in 6-well plates (100,000 cells/mL adherent; 200,000 cells/mL suspension) and treated with 0.75 mg/mL NG and then separated for the different substrates. After 24 h, adherent and suspension cells were harvested and lysed (300 μL of lysis buffer without protease inhibitor cocktail) similarly to preparations for Western blot analysis. After clarifying lysates, 30 μL of lysate was aliquoted in a new tube in the presence of 500 μL of general protease assay buffer (20 mM HEPES (pH 7.5), 10% glycerol, 0.5 mM EDTA) with 5 mM DTT and 20 μM of the relevant fluorogenic peptide substrates as above. Technical replicates (200 μL each) were plated in black 96-well plates, sealed, and incubated at 37 °C, 5% CO_2, by monitoring fluorescence as a function of time over 48 h.

■ ASSOCIATED CONTENT

Supporting Information

The Supporting Information is available free of charge at https://pubs.acs.org/doi/10.1021/jacsau.1c00261.

Materials and methods for synthesis and characterization of polymers as well as procedures for protein expression and purification, evaluation of caspase solvent exposed cysteines and NG characterization (encapsulation efficiencies, size evaluation, Cy5 labeling, and uptake study); supplemental Figures S1−S11, Tables S1−S3 and Scheme S1 (PDF)

■ AUTHOR INFORMATION

Corresponding Authors

Jeanne A. Hardy − *Department of Chemistry, University of Massachusetts, Amherst, Massachusetts 01003, United States;* orcid.org/0000-0002-3406-7997; Email: hardy@chem.umass.edu

S. Thayumanavan − *Department of Chemistry, University of Massachusetts, Amherst, Massachusetts 01003, United States;* orcid.org/0000-0002-6475-6726; Email: thai@chem.umass.edu

Author

Francesca Anson − *Department of Chemistry, University of Massachusetts, Amherst, Massachusetts 01003, United States*

Complete contact information is available at: https://pubs.acs.org/10.1021/jacsau.1c00261

Notes

The authors declare no competing financial interest.

■ ACKNOWLEDGMENTS

This work was supported by NIH R01 GM080532 and GM136395. F.A. was supported by the UMASS BTP Program (NIH T32 GM108556). We acknowledge Scott J. Eron and Witold A. Witkowski for supplying recombinant caspase proteins casp-9_{cD} and casp-7_{HC}. We acknowledge the Strieter lab for supplying proteasome inhibitor MG-132.

■ ABBREVIATIONS

caspase, casp, cysteine aspartate protease; NG, nanogel; BCL-2, B-cell lymphoma-2; IAP, inhibitors of apoptotic proteins; TNF, tumor necrosis factor; DED, death effector domain; DISC, death-inducing signaling complex; Apaf-1, apoptotic protease activating factor-1; CARD, caspase activation and recruitment domain; ISL, intersubunit linker; WT, wild-type; CT, constitutively two chain; LG, caspase large subunit; SM, caspase small subunit; pro, caspase prodomain; DTT, dithiothreitol; PEG, polyethylene glycol; PDS, pyridyl disulfide; PEG−PDS, polymer of PEG and PDS; 7-AAD, 7-aminoactinomycin; PBS, phosphate-buffered saline; SDS-PAGE, sodium dodecyl sulfate-polyacrylamide gel electrophoresis; GSH, glutathione; casp-9_{cD}, constitutively dimeric casp-9; casp-7_{HC}, handcuffed casp-7; PARP-1, poly(ADP-ribose) polymerase 1; DVL3, disheveled segment polarity protein 3; PARK7 or DJ-1, Parkinson's disease protein 7; BID and tBID (truncated BID), BH3 interacting-domain death agonist; HeLa-deGFP, HeLa cells expressing destabilized GFP

■ REFERENCES

(1) Reed, J. C. Apoptosis-Targeted Therapies for Cancer. *Cancer Cell* **2003**, *3*, 17−22.

(2) Boatright, K. M.; Salvesen, G. S. Mechanisms of Caspase Activation. *Curr. Opin. Cell Biol.* **2003**, *15*, 725−731.

(3) Walensky, L. D. BCL-2 in the Crosshairs: Tipping the Balance of Life and Death. *Cell Death Differ.* **2006**, *13*, 1339−1350.

(4) Riedl, S. J.; Shi, Y. Molecular Mechanisms of Caspase Regulation During Apoptosis. *Nat. Rev. Mol. Cell Biol.* **2004**, *5*, 897−907.

(5) Salvesen, G. S.; Duckett, C. S. IAP Proteins: Blocking the Road to Death's Door. *Nat. Rev. Mol. Cell Biol.* **2002**, *3*, 401−410.

(6) Wong, R. S. Y. Apoptosis in Cancer: From Pathogenesis to Treatment. *J. Exp. Clin. Cancer Res.* **2011**, *30*, 87.
(7) McStay, G. P.; Salvesen, G. S.; Green, D. R. Overlapping Cleavage Motif Selectivity of Caspases: Implications for Analysis of Apoptotic Pathways. *Cell Death Differ.* **2008**, *15*, 322−331.
(8) Zhivotovsky, B.; Samali, A.; Gahm, A.; Orrenius, S. Caspases: Their Intracellular Localization and Translocation during Apoptosis. *Cell Death Differ.* **1999**, *6*, 644−651.
(9) Prokhorova, E. A.; Kopeina, G. S.; Lavrik, I. N.; Zhivotovsky, B. Apoptosis Regulation by Subcellular Relocation of Caspases. *Sci. Rep.* **2018**, *8*, 12199.
(10) Ventura, J.; Eron, S. J.; González-Toro, D. C.; Raghupathi, K.; Wang, F.; Hardy, J. A.; Thayumanavan, S. Reactive Self-Assembly of Polymers and Proteins to Reversibly Silence a Killer Protein. *Biomacromolecules* **2015**, *16*, 3161−3171.
(11) Raghupathi, K.; Eron, S. J.; Anson, F.; Hardy, J. A.; Thayumanavan, S. Utilizing Inverse Emulsion Polymerization to Generate Responsive Nanogels for Cytosolic Protein Delivery. *Mol. Pharmaceutics* **2017**, *14*, 4515−4524.
(12) Siprashvili, Z.; Reuter, J. A.; Khavari, P. A. Intracellular Delivery of Functional Proteins via Decoration with Transporter Peptides. *Mol. Ther.* **2004**, *9*, 721−728.
(13) Zassler, B.; Blasig, I. E.; Humpel, C. Protein Delivery of Caspase-3 Induces Cell Death in Malignant C6 Glioma, Primary Astrocytes and Immortalized and Primary Brain Capillary Endothelial Cells. *J. Neuro-Oncol.* **2005**, *71*, 127−134.
(14) Hentzen, N. B.; Mogaki, R.; Otake, S.; Okuro, K.; Aida, T. Intracellular Photoactivation of Caspase-3 by Molecular Glues for Spatiotemporal Apoptosis Induction. *J. Am. Chem. Soc.* **2020**, *142*, 8080−8084.
(15) Fu, J.; Yu, C.; Li, L.; Yao, S. Q. Intracellular Delivery of Functional Proteins and Native Drugs by Cell-Penetrating Poly-disulfides. *J. Am. Chem. Soc.* **2015**, *137*, 12153−12160.
(16) Tang, R.; Kim, C. S.; Solfiell, D. J.; Rana, S.; Mout, R.; Velázquez-Delgado, E. M.; Chompoosor, A.; Jeong, Y.; Yan, B.; Zhu, Z. J.; Kim, C.; Hardy, J. A.; Rotello, V. M. Direct Delivery of Functional Proteins and Enzymes to the Cytosol Using Nanoparticle-Stabilized Nanocapsules. *ACS Nano* **2013**, *7*, 6667−6673.
(17) Kim, C. S.; Mout, R.; Zhao, Y.; Yeh, Y. C.; Tang, R.; Jeong, Y.; Duncan, B.; Hardy, J. A.; Rotello, V. M. Co-Delivery of Protein and Small Molecule Therapeutics Using Nanoparticle-Stabilized Nanocapsules. *Bioconjugate Chem.* **2015**, *26*, 950−954.
(18) Esteban-Fernández De Ávila, B.; Ramírez-Herrera, D. E.; Campuzano, S.; Angsantikul, P.; Zhang, L.; Wang, J. Nanomotor-Enabled PH-Responsive Intracellular Delivery of Caspase-3: Toward Rapid Cell Apoptosis. *ACS Nano* **2017**, *11*, 5367−5374.
(19) Boice, A.; Bouchier-Hayes, L. Targeting Apoptotic Caspases in Cancer. *Biochim. Biophys. Acta, Mol. Cell Res.* **2020**, *1867*, 118688.
(20) Yamabe, K.; Shimizu, S.; Ito, T.; Yoshioka, Y.; Nomura, M.; Narita, M.; Saito, I.; Kanegae, Y.; Matsuda, H. Cancer Gene Therapy Using a Pro-Apoptotic Gene, Caspase-3. *Gene Ther.* **1999**, *6*, 1952−1959.
(21) Chul Cho, K.; Hoon Jeong, J.; Jung Chung, H.; O Joe, C.; Wan Kim, S.; Gwan Park, T. Folate Receptor-Mediated Intracellular Delivery of Recombinant Caspase-3 for Inducing Apoptosis. *J. Controlled Release* **2005**, *108*, 121−131.
(22) Xie, X.; Zhao, X.; Liu, Y.; Zhang, J.; Matusik, R. J.; Slawin, K. M.; Spencer, D. M. Adenovirus-Mediated Tissue-Targeted Expression of a Caspase-9-Based Artificial Death Switch for the Treatment of Prostate Cancer. *Cancer Res.* **2001**, *61*, 6795−6804.
(23) Ando, M.; Hoyos, V.; Yagyu, S.; Tao, W.; Ramos, C. A.; Dotti, G.; Brenner, M. K.; Bouchier-Hayes, L. Bortezomib Sensitizes Non-Small Cell Lung Cancer to Mesenchymal Stromal Cell-Delivered Inducible Caspase-9-Mediated Cytotoxicity. *Cancer Gene Ther.* **2014**, *21*, 472−482.
(24) Zhang, X.; Turner, C.; Godbey, W. T. Comparison of Caspase Genes for the Induction of Apoptosis Following Gene Delivery. *Mol. Biotechnol.* **2009**, *41*, 236−246.
(25) Morales-Cruz, M.; Figueroa, C. M.; González-Robles, T.; Delgado, Y.; Molina, A.; Méndez, J.; Morales, M.; Griebenow, K. Activation of Caspase-Dependent Apoptosis by Intracellular Delivery of Cytochrome c-Based Nanoparticles. *J. Nanobiotechnol.* **2014**, *12*, 33.
(26) Dutta, K.; Hu, D.; Zhao, B.; Ribbe, A. E.; Zhuang, J.; Thayumanavan, S. Templated Self-Assembly of a Covalent Polymer Network for Intracellular Protein Delivery and Traceless Release. *J. Am. Chem. Soc.* **2017**, *139*, 5676−5679.
(27) Zhang, B.; Luo, Z.; Liu, J.; Ding, X.; Li, J.; Cai, K. Cytochrome c End-Capped Mesoporous Silica Nanoparticles as Redox-Responsive Drug Delivery Vehicles for Liver Tumor-Targeted Triplex Therapy in Vitro and in Vivo. *J. Controlled Release* **2014**, *192*, 192−201.
(28) Anson, F.; Liu, B.; Kanjilal, P.; Wu, P.; Hardy, J. A.; Thayumanavan, S. Evaluating Endosomal Escape of Caspase-3-Containing Nanomaterials Using Split GFP. *Biomacromolecules* **2021**, *22*, 1261−1272.
(29) Ryu, J.-H.; Chacko, R. T.; Jiwpanich, S.; Bickerton, S.; Babu, R. P.; Thayumanavan, S. Self-Cross-Linked Polymer Nanogels: A Versatile Nanoscopic Drug Delivery Platform. *J. Am. Chem. Soc.* **2010**, *132*, 17227−17235.
(30) Chacko, R. T.; Ventura, J.; Zhuang, J.; Thayumanavan, S. Polymer Nanogels: A Versatile Nanoscopic Drug Delivery Platform. *Adv. Drug Delivery Rev.* **2012**, *64*, 836−851.
(31) Salvesen, G. S.; Dixit, V. M. Caspase Activation : The Induced-Proximity Model. *Proc. Natl. Acad. Sci. U. S. A.* **1999**, *96*, 10964−10967.
(32) Shi, Y. Caspase Activation: Revisiting the Induced Proximity Model. *Cell* **2004**, *117*, 855−858.
(33) Cullen, S. P.; Martin, S. J. Caspase Activation Pathways: Some Recent Progress. *Cell Death Differ.* **2009**, *16*, 935−938.
(34) Simon, D. J.; Weimer, R. M.; Mclaughlin, T.; Kallop, D.; Stanger, K.; Yang, J.; O'Leary, D. D. M.; Hannoush, R. N.; Tessier-Lavigne, M. A Caspase Cascade Regulating Developmental Axon Degeneration. *J. Neurosci.* **2012**, *32*, 17540−17553.
(35) Slee, E. A.; Harte, M. T.; Kluck, R. M.; Wolf, B. B.; Casiano, C. A.; Newmeyer, D. D.; Wang, H.; Reed, J. C.; Nicholson, D. W.; Alnemri, E. S.; Green, D. R.; Martin, S. J. Ordering the Cytochrome c−Initiated Caspase Cascade: Hierarchical Activation of Caspases-2, −3, −6, −7, −8, and −10 in a Caspase-9−Dependent Manner. *J. Cell Biol.* **1999**, *144*, 281−292.
(36) McComb, S.; Chan, P. K.; Guinot, A.; Hartmannsdottir, H.; Jenni, S.; Dobay, M. P.; Bourquin, J. P.; Bornhauser, B. C. Efficient Apoptosis Requires Feedback Amplification of Upstream Apoptotic Signals by Effector Caspase-3 or −7. *Sci. Adv.* **2019**, *5*, eaau9433.
(37) Fujita, E.; Egashira, J.; Urase, K.; Kuida, K.; Momoi, T. Caspase-9 Processing by Caspase-3 via a Feedback Amplification Loop in Vivo. *Cell Death Differ.* **2001**, *8*, 335−344.
(38) Cowling, V.; Downward, J. Caspase-6 Is the Direct Activator of Caspase-8 in the Cytochrome c-Induced Apoptosis Pathway: Absolute Requirement for Removal of Caspase-6 Prodomain. *Cell Death Differ.* **2002**, *9*, 1046−1056.
(39) Inoue, S.; Browne, G.; Melino, G.; Cohen, G. M. Ordering of Caspases in Cells Undergoing Apoptosis by the Intrinsic Pathway. *Cell Death Differ.* **2009**, *16*, 1053−1061.
(40) Brentnall, M.; Rodriguez-Menocal, L.; De Guevara, R.; Cepero, E.; Boise, L. H Caspase-9, Caspase-3 and Caspase-7 Have Distinct Roles during Intrinsic Apoptosis. *BMC Cell Biol.* **2013**, *14*, 32.
(41) Stennicke, H. R.; Jürgensmeier, J. M.; Shin, H.; Deveraux, Q.; Wolf, B. B.; Yang, X.; Zhou, Q.; Ellerby, H. M.; Ellerby, L. M.; Bredesen, D.; Green, D. R.; Reed, J. C.; Froelich, C. J.; Salvesen, G. S. Pro-Caspase-3 Is a Major Physiologic Target of Caspase-8. *J. Biol. Chem.* **1998**, *273*, 27084−27090.
(42) Li, H.; Zhu, H.; Xu, C. J.; Yuan, J. Cleavage of BID by Caspase 8 Mediates the Mitochondrial Damage in the Fas Pathway of Apoptosis. *Cell* **1998**, *94*, 491−501.
(43) Kantari, C.; Walczak, H. Caspase-8 and Bid: Caught in the Act between Death Receptors and Mitochondria. *Biochim. Biophys. Acta, Mol. Cell Res.* **2011**, *1813*, 558−563.

https://doi.org/10.1021/jacsau.1c00261
JACS Au 2021, 1, 1240−1256

(44) Allsopp, T. E.; McLuckie, J.; Kerr, L. E.; Macleod, M.; Sharkey, J.; Kelly, J. S. Caspase 6 Activity Initiates Caspase 3 Activation in Cerebellar Granule Cell Apoptosis. *Cell Death Differ.* **2000**, *7*, 984−993.
(45) Walsh, J. G.; Cullen, S. P.; Sheridan, C.; Lüthi, A. U.; Gerner, C.; Martin, S. J. Executioner Caspase-3 and Caspase-7 Are Functionally Distinct Proteases. *Proc. Natl. Acad. Sci. U. S. A.* **2008**, *105*, 12815−12819.
(46) Van De Craen, M.; Declercq, W.; Van Den Brande, I.; Fiers, W.; Vandenabeele, P. The Proteolytic Procaspase Activation Network: An in Vitro Analysis. *Cell Death Differ.* **1999**, *6*, 1117−1124.
(47) Ferrall-Fairbanks, M. C.; Kieslich, C. A.; Platt, M. O. Reassessing Enzyme Kinetics: Considering Protease-as-Substrate Interactions in Proteolytic Networks. *Proc. Natl. Acad. Sci. U. S. A.* **2020**, *117*, 3307−3318.
(48) Duclos, C.; Lavoie, C.; Denault, J. B. Caspases Rule the Intracellular Trafficking Cartel. *FEBS J.* **2017**, *284*, 1394−1420.
(49) Dagbay, K. B.; Hill, M. E.; Barrett, E.; Hardy, J. A. Tumor-Associated Mutations in Caspase-6 Negatively Impact Catalytic Efficiency. *Biochemistry* **2017**, *56*, 4568−4577.
(50) Shen, C.; Pei, J.; Guo, X.; Zhou, L.; Li, Q.; Quan, J. Structural Basis for Dimerization of the Death Effector Domain of the F122A Mutant of Caspase-8. *Sci. Rep.* **2018**, *8*, 16723.
(51) Dagbay, K. B.; Hardy, J. A. Multiple Proteolytic Events in Caspase-6 Self-Activation Impact Conformations of Discrete Structural Regions. *Proc. Natl. Acad. Sci. U. S. A.* **2017**, *114*, E7977−E7986.
(52) Donepudi, M.; Sweeney, A. M.; Briand, C.; Grutter, M. G Insights into the Regulatory Mechanism for Caspase-8 Activation. *Mol. Cell* **2003**, *11*, 543−549.
(53) Huber, K. L.; Serrano, B. P.; Hardy, J. A. Caspase-9 CARD: Core Domain Interactions Require a Properly Formed Active Site. *Biochem. J.* **2018**, *475*, 1177−1196.
(54) Ryu, J. H.; Jiwpanich, S.; Chacko, R.; Bickerton, S.; Thayumanavan, S. Surface-Functionalizable Polymer Nanogels with Facile Hydrophobic Guest Encapsulation Capabilities. *J. Am. Chem. Soc.* **2010**, *132*, 8246−8247.
(55) Canakci, M.; Singh, K.; Munkhbat, O.; Shanthalingam, S.; Mitra, A.; Gordon, M.; Osborne, B. A.; Thayumanavan, S. Targeting CD4+ Cells with Anti-CD4 Conjugated Mertansine-Loaded Nanogels. *Biomacromolecules* **2020**, *21*, 2473−2481.
(56) Garcia-Calvo, M.; Peterson, E. P.; Rasper, D. M.; Vaillancourt, J. P.; Zamboni, R.; Nicholson, D. W.; Thornberry, N. A. Purification and Catalytic Properties of Human Caspase Family Members. *Cell Death Differ.* **1999**, *6*, 362−369.
(57) Chao, Y.; Shiozaki, E. N.; Srinivasula, S. M.; Rigotti, D. J.; Fairman, R.; Shi, Y. Engineering a Dimeric Caspase-9: A Re-Evaluation of the Induced Proximity Model for Caspase Activation. *PLoS Biol.* **2005**, *3*, e183.
(58) Dagbay, K.; Eron, S. J.; Serrano, B. P.; Velázquez-Delgado, E. M.; Zhao, Y.; Lin, D.; Vaidya, S.; Hardy, J. A. A Multi-Pronged Approach for Compiling a Global Map of Allosteric Regulation in the Apoptotic Caspases. *Methods Enzymol.* **2014**, *544*, 215−249.
(59) Boucher, D.; Blais, V.; Denault, J. B. Caspase-7 Uses an Exosite to Promote Poly(ADP Ribose) Polymerase 1 Proteolysis. *Proc. Natl. Acad. Sci. U. S. A.* **2012**, *109*, 5669−5674.
(60) MacPherson, D. J.; Mills, C. L.; Ondrechen, M. J.; Hardy, J. A. Tri-Arginine Exosite Patch of Caspase-6 Recruits Substrates for Hydrolysis. *J. Biol. Chem.* **2019**, *294*, 71−88.
(61) Anson, F.; Kanjilal, P.; Thayumanavan, S.; Hardy, J. A. Tracking Exogenous Intracellular Casp-3 Using Split GFP. *Protein Sci.* **2021**, *30*, 366−380.
(62) Oliver, F. J.; De La Rubia, G.; Rolli, V.; Ruiz-Ruiz, M. C.; De Murcia, G.; Ménissier-De Murcia, J. Importance of Poly(ADP-Ribose) Polymerase and Its Cleavage in Apoptosis: Lesson from an Uncleavable Mutant. *J. Biol. Chem.* **1998**, *273*, 33533−33539.
(63) Klaiman, G.; Champagne, N.; LeBlanc, A. C. Self-Activation of Caspase-6 in Vitro and in Vivo: Caspase-6 Activation Does Not Induce Cell Death in HEK293T Cells. *Biochim. Biophys. Acta, Mol. Cell Res.* **2009**, *1793*, 592−601.
(64) Hill, M. E.; MacPherson, D. J.; Wu, P.; Julien, O.; Wells, J. A.; Hardy, J. A. Reprogramming Caspase-7 Specificity by Regio-Specific Mutations and Selection Provides Alternate Solutions for Substrate Recognition. *ACS Chem. Biol.* **2016**, *11*, 1603−1612.
(65) Benchoua, A.; Couriaud, C.; Guéagan, C.; Tartier, L.; Couvert, P.; Friocourt, G.; Chelly, J.; Meanissier-de Murcia, J.; Ontéaniente, B. Active Caspase-8 Translocates into the Nucleus of Apoptotic Cells to Inactivate Poly(ADP-Ribose) Polymerase-2. *J. Biol. Chem.* **2002**, *277*, 34217−34222.
(66) Desroches, A.; Denault, J. B. Caspase-7 Uses RNA to Enhance Proteolysis of Poly(ADP-Ribose) Polymerase 1 and Other RNA-Binding Proteins. *Proc. Natl. Acad. Sci. U. S. A.* **2019**, *116*, 21521−21528.
(67) Wlodkowic, D.; Telford, W.; Skommer, J.; Darzynkiewicz, Z. Apoptosis and Beyond: Cytometry in Studies of Programmed Cell Death. *Methods Cell Biol.* **2011**, *103*, 55−98.
(68) Valenzuela, M. M. A.; Ferguson Bennit, H. R.; Gonda, A.; Diaz Osterman, C. J.; Hibma, A.; Khan, S.; Wall, N. R. Exosomes Secreted from Human Cancer Cell Lines Contain Inhibitors of Apoptosis (IAP). *Cancer Microenviron.* **2015**, *8*, 65−73.
(69) Tamm, I.; Kornblau, S. M.; Segall, H.; Krajewski, S.; Welsh, K.; Kitada, S.; Scudiero, D. A.; Tudor, G.; Qui, Y. H.; Monks, A.; Andreeff, M.; Reed, J. C. Expression and Prognostic Significance of IAP-Family Genes in Human Cancers and Myeloid Leukemias. *Clin. Cancer Res.* **2000**, *6*, 1796−1803.
(70) Paul, A.; Krelin, Y.; Arif, T.; Jeger, R.; Shoshan-Barmatz, V. A New Role for the Mitochondrial Pro-Apoptotic Protein SMAC/Diablo in Phospholipid Synthesis Associated with Tumorigenesis. *Mol. Ther.* **2018**, *26*, 680−694.
(71) Fakler, M.; Loeder, S.; Vogler, M.; Schneider, K.; Jeremias, I.; Debatin, K. M.; Fulda, S. Small Molecule XIAP Inhibitors Cooperate with TRAIL to Induce Apoptosis in Childhood Acute Leukemia Cells and Overcome Bcl-2-Mediated Resistance. *Blood* **2009**, *113*, 1710−1722.
(72) Suzuki, Y.; Nakabayashi, Y.; Nakata, K.; Reed, J. C.; Takahashi, R. X-Linked Inhibitor of Apoptosis Protein (XIAP) Inhibits Caspase-3 and −7 in Distinct Modes. *J. Biol. Chem.* **2001**, *276*, 27058−27063.
(73) Shiozaki, E. N.; Chai, J.; Rigotti, D. J.; Riedl, S. J.; Li, P.; Srinivasula, S. M.; Alnemri, E. S.; Fairman, R.; Shi, Y. Mechanism of XIAP-Mediated Inhibition of Caspase-9. *Mol. Cell* **2003**, *11*, 519−527.
(74) Choi, Y. E.; Butterworth, M.; Malladi, S.; Duckett, C. S.; Cohen, G. M.; Bratton, S. B. The E3 Ubiquitin Ligase CIAP1 Binds and Ubiquitinates Caspase-3 and −7 via Unique Mechanisms at Distinct Steps in Their Processing. *J. Biol. Chem.* **2009**, *284*, 12772−12782.
(75) Eckelman, B. P.; Salvesen, G. S. The Human Anti-Apoptotic Proteins CIAP1 and CIAP2 Bind but Do Not Inhibit Caspases. *J. Biol. Chem.* **2006**, *281*, 3254−3260.
(76) Guicciardi, M. E.; Mott, J. L.; Bronk, S. F.; Kurita, S.; Fingas, C. D.; Gores, G. J. Cellular Inhibitor of Apoptosis 1 (CIAP-1) Degradation by Caspase 8 During TNF-Related Apoptosis-Inducing Ligand (TRAIL)-Induced Apoptosis. *Exp. Cell Res.* **2011**, *317*, 107−116.
(77) Wu, G.; Chai, J.; Suber, T. L.; Wu, J. W.; Du, C.; Wang, X.; Shi, Y. Structural Basis of IAP Recognition by Smac/DIABLO. *Nature* **2000**, *408*, 1008−1012.
(78) Placzek, W. J.; Wei, J.; Kitada, S.; Zhai, D.; Reed, J. C.; Pellecchia, M. A Survey of the Anti-Apoptotic Bcl-2 Subfamily Expression in Cancer Types Provides a Platform to Predict the Efficacy of Bcl-2 Antagonists in Cancer Therapy. *Cell Death Dis.* **2010**, *1*, e40−9.
(79) Zembruski, N. C. L.; Stache, V.; Haefeli, W. E.; Weiss, J. 7-Aminoactinomycin D for Apoptosis Staining in Flow Cytometry. *Anal. Biochem.* **2012**, *429*, 79−81.
(80) Lecoeur, H.; De Oliveira-Pinto, L. M.; Gougeon, M. L. Multiparametric Flow Cytometric Analysis of Biochemical and Functional Events Associated with Apoptosis and Oncosis Using the 7-Aminoactinomycin D Assay. *J. Immunol. Methods* **2002**, *265*, 81−96.
(81) Liu, B.; Ejaz, W.; Kurbanov, M.; Gong, S.; Canakci, M.; Anson, F.; Thayumanavan, S. Engineered Interactions with Mesoporous Silica Facilitate Intracellular Delivery of Proteins and Gene Editing. *Nano Lett.* **2020**, *20*, 4014−4021.

https://doi.org/10.1021/jacsau.1c00261
JACS Au 2021, 1, 1240−1256

(82) Strebel, A.; Harr, T.; Bachmann, F.; Wernli, M.; Erb, P. Green Fluorescent Protein as a Novel Tool to Measure Apoptosis and Necrosis. *Cytometry* **2001**, *43*, 126−133.
(83) Witkowski, W. A.; Hardy, J. A. A Designed Redox-Controlled Caspase. *Protein Sci.* **2011**, *20*, 1421−1431.
(84) Tenev, T.; Marani, M.; McNeish, I.; Lemoine, N. R. Pro-Caspase-3 Overexpression Sensitises Ovarian Cancer Cells to Proteasome Inhibitors. *Cell Death Differ.* **2001**, *8*, 256−264.
(85) Guo, N.; Peng, Z. MG132, a Proteasome Inhibitor, Induces Apoptosis in Tumor Cells. *Asia. Pac. J. Clin. Oncol.* **2013**, *9*, 6−11.
(86) Julien, O.; Wells, J. A. Caspases and Their Substrates. *Cell Death Differ.* **2017**, *24*, 1380−1389.
(87) Shete, H. K.; Prabhu, R. H.; Patravale, V. B. Endosomal Escape: A Bottleneck in Intracellular Delivery. *J. Nanosci. Nanotechnol.* **2014**, *14*, 460−474.
(88) Smith, S. A.; Selby, L. I.; Johnston, A. P. R.; Such, G. K. The Endosomal Escape of Nanoparticles: Toward More Efficient Cellular Delivery. *Bioconjugate Chem.* **2019**, *30*, 263−272.
(89) Lopes, R. B.; Gangeswaran, R.; McNeish, I. A.; Wang, Y.; Lemoine, N. R. Expression of the IAP Protein Family Is Dysregulated in Pancreatic Cancer Cells and Is Important for Resistance to Chemotherapy. *Int. J. Cancer* **2007**, *120*, 2344−2352.
(90) Endo, T.; Abe, S.; Seidlar, H. B. K.; Nagaoka, S.; Takemura, T.; Utsuyama, M.; Kitagawa, M.; Hirokawa, K. Expression of IAP Family Proteins in Colon Cancers from Patients Will Different Age Groups. *Cancer Immunol. Immunother.* **2004**, *53*, 770−776.
(91) Tirrò, E.; Consoli, M. L.; Massimino, M.; Manzella, L.; Frasca, F.; Sciacca, L.; Vicari, L.; Stassi, G.; Messina, L.; Messina, A.; Vigneri, P. Altered Expression of C-IAP1, Survivin, and Smac Contributes to Chemotherapy Resistance in Thyroid Cancer Cells. *Cancer Res.* **2006**, *66*, 4263−4272.
(92) Eron, S. J.; MacPherson, D. J.; Dagbay, K. B.; Hardy, J. A. Multiple Mechanisms of Zinc-Mediated Inhibition for the Apoptotic Caspases-3, −6, −7, and −8. *ACS Chem. Biol.* **2018**, *13*, 1279−1290.
(93) Yang, L.; Cao, Z.; Yan, H. Coexistence of High Levels of Apoptotic Signaling and Inhibitor of Apoptosis Proteins in Human Tumor Cells. *Cancer Res.* **2003**, *63*, 6815−6824.
(94) Eron, S. J.; Raghupathi, K.; Hardy, J. A. Dual Site Phosphorylation of Caspase-7 by PAK2 Blocks Apoptotic Activity by Two Distinct Mechanisms. *Structure* **2017**, *25*, 27−39.
(95) Huang, Z.; Pinto, J. T.; Deng, H.; Richie, J. P. Inhibition Of Caspase-3 Activity and Activation by Protein Glutathionylation. *Biochem. Pharmacol.* **2008**, *75*, 2234−2244.
(96) Kivinen, K.; Kallajoki, M.; Taimen, P. Caspase-3 Is Required in the Apoptotic Disintegration of the Nuclear Matrix. *Exp. Cell Res.* **2005**, *311*, 62−73.
(97) Van Engeland, M.; Nieland, L. J. W.; Ramaekers, F. C. S.; Schutte, B.; Reutelingsperger, C. P. M. Annexin V-Affinity Assay: A Review on an Apoptosis Detection System Based on Phosphatidylserine Exposure. *Cytometry* **1998**, *31*, 1−9.

https://doi.org/10.1021/jacsau.1c00261
JACS Au 2021, 1, 1240−1256